Chapter 5

Chapter 5 Prediction of Air Quality by Air Quality Simulation Model

5.1 Outline of the Air Quality Models

5.1.1 Objective

The Study area for this project is the entire country of Macedonia. However, for the modeling effort, the simulation modeling has been limited to one city. The city selected for the simulation modeling is Skopje with some 60-70 major and mid-size point sources which contribute to the air pollution problem.
Air simulation modeling provides a rational (scientifically-based) method for estimating source contributions, which can then be used to determine the effectiveness of emission reduction alternatives in meeting Macedonian ambient air quality objectives. The method can also be applied numerous times to answer "what if" question for future year emission changes. In the Study the objectives were to develop an example modeling approach and methodology which could be used by Macedonian counterparts;

- as a basis upon which further refinements to modeling could be developed,
- to examine control strategy effectiveness in meeting air quality objectives,
- to develop similar approaches for other cities within Macedonia.

To meet these objectives, air quality modeling study was performed for Skopje, for a base year (1998), one future-year (2008) without additional control measures, and one future-year (2008) with implementation of control measures.

5.1.2 Modeling Approach

Two general classes of air quality models were used in the Study. An air quality dispersion model which simulates the dispersion of air pollutants once they are released into the environment by simulating all of the physical process which take place in the atmosphere (dispersion, transport, deposition, chemical transformation). By simulating these physical processes for all sources of pollutants the model can detail emission source contributions. However, the model is dependent upon reliable measures of emissions and meteorology. Emission estimates are usually reasonably known for CO, SO_2 and NO_2, but are often poorly known for SPM. To strengthen the conclusions regarding SPM source contribution from the dispersion model a receptor

model is used to confirm/support the conclusion. A receptor model examines ambient measurement of SPM for their chemical constituents and compares observed chemical composition to those of emission source profiles to establish source contribution. To successfully apply the method with a high degree of confidence requires many ambient measurement samples and their subsequent chemical analysis and emission source profile information.

(1) Dispersion Modeling Approach

1) Long-term Modeling

To simulate the annual average concentration for the pollutants of; sulfur dioxide (SO_2), suspended particulate matter (SPM), carbon monoxide (CO) and nitrogen dioxide (NO_2). Four candidate air quality dispersion models were considered for this Study. These were ISC3, AERMOD, SHORTZ and CALPUFF. The Industrial Source Complex 3 (ISC3) is the current USEPA recommended guideline model for modeling complex industrial source settings and has undergone extensive model evaluation. It is capable of modeling areas of up to 50 km between source and receptor. In addition, the model has been optimized for running in long-term mode. Hence, the ISC3-LT (long-term version) was selected for the annual average modeling (Ref. 5-1).

a) The ISC Long-term Dispersion Model Equations

The ISC Long-term Model uses input meteorological data that have been summarized into joint frequencies of occurrence for particular wind speed classes, wind direction sectors, and stability categories. These summaries, called STAR summaries for STability ARray, may include frequency distributions over a monthly, seasonal or annual basis. The long-term model has the option of calculating concentration or dry deposition values for each separate STAR summary input and/or for the combined period covered by all available STAR summaries. Since the wind direction input is the frequency of occurrence over a sector, with no information on the distribution of winds within the sector, the ISC Long-term Model uses a Gaussian sector-average plume equation as the basis for modeling pollutant emissions on a long-term basis.

i) Point Source Emissions

① The Gaussian Sector Average Equation

In the long-term model, the area surrounding a continuous source of pollutants is divided into sectors of equal angular width corresponding to the sectors of the

seasonal and annual frequency distributions of wind direction, wind speed, and stability. Seasonal or annual emissions from the source are partitioned among the sectors according to the frequencies of wind blowing toward the sectors. The concentration fields calculated for each source are translated to a common coordinate system and summed to obtain the total due to all sources.

For a single stack, the mean seasonal concentration is given by:

$$\chi_l = \frac{K}{\sqrt{2\pi}\ R\Delta\theta'} \sum_{i,j,k} \frac{QfSVD}{u_s\sigma_z} \qquad (1\text{-}1)$$

where,

K: units scaling coefficient to convert calculated concentrations to desired units (default value of 1×10^6 for Q in g/s and concentration in $\mu g/m^3$)

Q: pollutant emission rate (mass per unit time), for the i^{th} wind speed category, the k^{th} stability category and the l^{th} season

f: frequency of occurrence of the i^{th} wind speed category, the j^{th} wind direction category and the k^{th} stability category for the l^{th} season

θ': the sector width in radians

R: radial distance from lateral virtual point source (building downwash) to the receptor = $[(x+x_y)^2 + y^2]^{1/2}$ (m)

x: downwind distance from source center to receptor, measured along the plume axis (m)

y: lateral distance from the plume axis to the receptor (m)

x_y: lateral virtual distance, equals zero for point sources without building downwash, and for downwash sources that do not experience lateral dispersion enhancement (m)

S: a smoothing function similar to that of the Air Quality Dispersion Model (AQDM)

u_s: mean wind speed (m/sec) at stack height for the i^{th} wind speed category and k^{th} stability category

σ_z: standard deviation of the vertical concentration distribution (m) for the k^{th} stability category

V: the Vertical Term for the i^{th} wind speed category, k^{th} stability category and l^{th} season

D: the Decay Term for the i^{th} wind speed category and k^{th} stability category

The mean annual concentration at the point is calculated from the seasonal concentrations using the expression:

$$\chi_a = 0.25 \sum_{l=1}^{4} \chi_l \qquad (1\text{-}2)$$

② Basic Plume Rise Equations

The basic point source plume rise relationships are based on the Briggs (1975) equations. The plume rise due to buoyancy and momentum during neutral or unstable conditions, z_n is:

$$z_n = \left[3 F_m x / \left(\beta_j^2 u_s^2\right) + 3 F x^2 / \left(2 \beta_1^2 u_s^3\right)\right]^{1/3} \qquad (1\text{-}3)$$

where,

F_m: the momentum flux (m^4/s^2)

F: the buoyancy flux (m^4/s^3)

u_s: the stack height wind speed (m/s)

x: the downwind distance (m)

β_1: the neutral entrainment parameter (~ 0.6)

β_j: the jet entrainment coefficient ($_j$ = 1/3 + us/w)

w: the stack gas exit speed (m/s)

The distance to final plume rise, χ_f, is:

$$x_f = \begin{cases} 3.5 x^* & F > 0 \\ 4D \left(w + 3 u_s\right)^2 / \left(u_s w\right) & F = 0 \end{cases} \qquad (1\text{-}4)$$

$$x^{*} = \begin{cases} 14\ F^{5/8} & F \le 55 m^4/s^3 \\ 34\ F^{2/5} & F > 55\ m^4/s^3 \end{cases} \quad (1\text{-}5)$$

where,

D: the stack diameter (m)

During stable conditions, the final plume rise, z_{sf}, is determined by:

$$z_{sf} = \left[3 F_m / \left(\beta_j^2 u_s S^{1/2}\right) + 6F / \left(\beta_2^2 u_s S\right)\right]^{1/3} \quad (1\text{-}6)$$

where,

β: the stable entrainment parameter (~ 0.6)

S: a stability parameter [(g/Ta)(dθ/dz)

g: the acceleration due to gravity (m/s^2)

Ta: the ambient temperature (deg. K)

dθ/dz: the potential temperature lapse rate (deg. K/m)

ii) Non-point Source Emissions

The ISC Long-term Area Source Model is based on the numerical integration algorithm for modeling area sources used by the ISC Short-term Model for each combination of wind speed class, stability category and wind direction sector in the STAR meteorological frequency summary, the ISC Long-term Model calculates a sector average concentration by integrating the results from the ISC Short-term Model area source algorithm across the sector. A trapezoidal integration is used, as follows:

$$\overline{\chi_i} = \frac{\int f(\theta)\chi(\theta)\,d\theta}{S} = \frac{1}{N}\left[\sum_{j=1}^{N-1} f_{ij}\chi(\theta_{ij}) + \frac{\left(f_{i1}\chi(\theta_{i1}) + f_{iN}\chi(\theta_{iN})\right)}{2}\right] + \varepsilon(\theta) \quad (1\text{-}7)$$

$$\varepsilon(\theta) = \frac{\overline{\chi_{NEW}} - \overline{\chi_{OLD}}}{\overline{\chi_{mid}}}\ ;\ \overline{\chi_{mid}} = \frac{\overline{\chi_{NEW}} + \overline{\chi_{OLD}}}{2} \quad (1\text{-}8)$$

where,

$\bar{\chi}_i$: the sector average concentration value for the i^{th} sector

S : the sector width

f_{ij}: the frequency of occurrence for the j^{th} wind direction in the i^{th} sector

$\varepsilon(\theta)$: the error term - a criterion of $\varepsilon(\theta) < 2$ percent is used to check for convergence of the sector average calculation

$\chi(\theta_{ij})$: the concentration value, based on the numerical integration algorithm for the j^{th} wind direction in the i^{th} sector

θ_{ij}: the j^{th} wind direction in the i^{th} sector, j = 1 and N correspond to the two boundaries of the sector

2) Short-term Modeling

Another goal for the modeling was to simulate hourly SO_2 concentrations for a typical SO_2 episode of 3-4 day duration. Two candidate models were considered for this effort; the Urban Airshed Model (UAM) and CALPUFF modeling systems.
The CALPUFF model was selected as the preferred modeling approach for this location (Ref. 5-2).

a) The CULPUFF Model Equation

CALPUFF contains algorithms for near-source effects such as building downwash, transitional plume rise, partial plume penetration, subgrid scale terrain interactions as well as longer range effects such as pollutant removal (wet scavenging and dry deposition), chemical transformation, vertical wind shear, overwater transport and coastal interaction effects. It can accommodate arbitrarily-varying point source and gridded area source emissions.

The basic equation for the contribution of a puff at a receptor is:

$$C = \frac{Q}{2\pi\sigma_x\sigma_y} g \exp\left[-d_a^2/\left(2\sigma_x^2\right)\right] \exp\left[-d_c^2/\left(2\sigma_y^2\right)\right] \quad (2\text{-}1)$$

$$g = \frac{2}{(2\pi)^{1/2}\sigma_z} \sum_{n=-\infty}^{\infty} \exp\left[-\left(H_e + 2nh\right)^2/\left(2\sigma_z^2\right)\right] \quad (2\text{-}2)$$

where,

C: the ground-level concentration (g/m^3)

Q: the pollutant mass (g) in the puff

σ_x: the standard deviation (m) of the Gaussian distribution in the along-wind direction

σ_y: the standard deviation (m) of the Gaussian distribution in the cross-wind direction

σ_z: the standard deviation (m) of the Gaussian distribution in the vertical direction

d_a: the distance (m) from the puff center to the receptor in the along-wind direction

d_c: the distance (m) from the puff center to the receptor in the cross-wind direction

g: the vertical term (m) of the Gaussian equation

H_e: the effective height (m) above the ground of the puff center

h: the mixed-layer height (m)

The summation in the vertical term, g, accounts for multiple reflections off the mixing lid and the ground. It reduces to the uniformly mixed limit of 1/h for $\sigma_z > 1.6$ h. In general, puffs within the convective boundary layer meet this criterion within a few hours after release.

For a horizontally symmetric puff, with $\sigma_x = \sigma_y$, Eqn. (2-1) reduces to:

$$C(s) = \frac{Q(s)}{2\pi\sigma_y^2(s)}\, g(s)\, \exp\left[-R^2(s) / \left(2\sigma_y^2(s)\right)\right] \qquad (2\text{-}3)$$

where,

R: the distance (m) from the center of the puff to the receptor

s: the distance (m) traveled by the puff

The distance dependence of the variables in Eqn. (2-3) is indicated (e.g., C (s), σ_y (s), etc.). Integrating Eqn. (2-3) over the distance of puff travel, ds, during the sampling step, dt, yields the time averaged concentration,C.

$$\overline{C} = \frac{1}{ds}\int_{s_o}^{s_o+ds} \frac{Q(s)}{2\pi\sigma_y^{\,2}(s)}\, g(s)\, \exp\left[-R^2(s)/2\sigma_y^2(s)\right] ds \qquad (2\text{-}4)$$

where,

s_o: the value of s at the beginning of the sampling step

The major feature and options of the CALPUFF model are summarized in Table 5.1, and summary of input data used by CALPUFF are shown in Table 5.2.

Table 5.1 (1) Major Features of the CALPUFF Model

- **Source Types**
  - · Point sources (constant or variable emissions)
  - · Line sources (constant emissions)
  - · Volume sources (constant or variable emissions)
  - · Area sources (constant or variable emissions)
- **Non-Steady-state Emissions and Meteorological Conditions**
  - · Gridded 3-D fields of meteorological variables (winds, temperature)
  - · Spatially-variable fields of mixing height, friction velocity, convective velocity scale, Monin-Obukhov length, precipitation rate
  - · Vertically and horizontally-varying turbulence and dispersion rates
  - · Time-dependent source and emissions data
- **Efficient Sampling Functions**
  - · Integrated puff formulation
  - · Elongated puff (slug) formulation
- **Dispersion Coefficient (σ_y, σ_z) Options**
  - · Direct measurements of σ_v and σ_w
  - · Estimated values of σ_v and σ_w based on similarity theory
  - · Pasquill-Gifford (PG) dispersion coefficients (rural areas)
  - · McElroy-Pooler (MP) dispersion coefficients (urban areas)
- **Vertical Wind Shear**
  - · Puff splitting
  - · Differential advection and dispersion
- **Plume Rise**
  - · Partial penetration
  - · Buoyant and momentum rise
  - · Stack tip effects
  - · Vertical wind shear
  - · Building downwash effects
- **Building Downwash**
  - · Huber-Snyder method
  - · Schulman-Scire method

Table 5.1 (2) Major Features of the CALPUFF Model

- **Subgrid Scale Complex Terrain**
  - Dividing streamline, Hd:
    - -Above Hd, puff flows over the hill and experiences altered diffusion rates
    - -Below Hd, puff deflects around the hill, splits, and wraps around the hill
- **Interface to the Emissions Production Model (EPM)**
  - Time-varying heat flux and emissions from controlled burns and wildfires
- **Dry Deposition**
  - Gases and particulate matter
  - Three options:
    - -Full treatment of space and time variations of deposition with a resistance model
    - -User-specified diurnal cycles for each pollutant
    - -No dry deposition
- **Overwater and Coastal Interaction Effects**
  - Overwater boundary layer parameters
  - Abrupt change in meteorological conditions, plume dispersion at coastal boundary
  - Plume fumigation
- **Chemical Transformation Options**
  - Pseudo-first-order chemical mechanism for SO_2, SO, NO_x, HNO_3, and NO (MESOPUFF II method)
  - User-specified diurnal cycles of transformation rates
  - No chemical conversion
- **Wet Removal**
  - Scavenging coefficient approach
  - Removal rate a function of precipitation intensity and precipitation type
- **Graphical User Interface**
  - Click-and-point model setup and data input
  - Enhanced error checking of model inputs
  - On-line Help files

Table 5.2 Summary of Input Data Used by CALPUFF

- **Geophysical Data (CALMET.DAT)**
  - Gridded fields of:
    - surface roughness lengths (z_o)
    - land use categories
    - terrain elevations
    - leaf area indices
- **Meteorological Data (CALMET.DAT)**
  - Gridded fields of:
    - u, v, w wind components (3-D)
    - air temperature (3-D)
    - surface friction velocity (u_*)
    - convective velocity scale (w_*)
    - mixing height (z_i)
    - Monin-Obukhov length (L)
    - PGT stability class
    - Precipitation rate
  - Hourly values of the following parameters at surface meteorological stations:
    - air density (ρ_a)
    - air temperature
    - short-wave solar radiation
    - relative humidity
    - precipitation type
- **Emissions Data**
  - Point source emissions:
    - Source and emissions data for point sources with constant emission parameters (CALPUFF. INP)
    - Source and emissions data for point sources with arbitrarily-varying emission parameters (PTEMARB. DAT)
  - Area source emissions
    - Emissions and initial size, height, and location for area sources with constant emission parameters (CALPUFF. INP)
    - Gridded emissions data for buoyant area sources with time-varying emission parameters (BAEMARB. DAT)
  - Volume source emissions
    - Emissions, height, size, and location of volume sources with constant emission parameters (CALPUFF. INP)
    - Emissions data for volume sources with time-varying emission parameters (VOLEM. DAT)
  - Line source emissions
    - Source and emissions data, height, length, location, spacing, and orientation of line sources with constant emission parameters (CALPUFF. INP)
- **Deposition Velocity Data (VD. DAT)**
  - Deposition velocity for each user-specified species for each hour of a diurnal cycle
- **Ozone Monitoring Data (OZONE. DAT)**
  - Hourly ozone measurements at one or more monitoring stations
- **Chemical Transformation Data (CHEM. DAT)**
  - Species-dependent chemical transformation rates for each hour of a diurnal cycle
- **Turbulence Observational Data (SIGMA. DAT)**
  - Hourly measurements of turbulence (σ_v, σ_w) at an onsite meteorological tower
- **Hill Data (HILL. DAT)**
  - Hill shape and height parameters for use in the subgrid-scale complex terrain module (CTSG)

b) Related Models

The CALMET meteorological model consists of a diagnostic wind field module and micrometeorological modules for overwater and overland boundary layers. When using large domains, the user has the option to adjust input winds to a Lambert Conformal Projection coordinate system to account for Earth's curvature. The diagnostic wind field module uses a two step approach to the computation of the wind fields (Douglas and Kessler, 1988). In the first step, an initial-guess wind field is adjusted for kinematic effects of terrain, slope flows, and terrain blocking effects to produce a Step one wind field. The second step consists of an objective analysis procedure to introduce observational data into the Step one wind field to produce a final wind field. An option is provided to allow gridded prognostic wind fields to be used by CALMET, which may better represent regional flows and certain aspects of sea breeze circulations and slope/valley circulations. Wind fields generated by the CSUMM prognostic wind field module can be input to CALMET as either the initial guess field or the Step one wind field (Ref. 5-3).

The major features and options of the meteorological model are summarized in Table 5.3.

Table 5.3 Major Features of the CALMET and CSUMM Meteorological Models

Boundary Layer Modules of CALMET

- Overland Boundary Layer - Energy Balance Method
- Overwater Boundary Layer - Profile Method
- Produces Gridded Fields of:
  - Surface Friction Velocity
  - Convective Velocity Scale
  - Monin-Obukhov Length
  - Mixing Height
  - PGT Stability Class
  - Air Temperature (3-D)
  - Precipitation Rate

Diagnostic Wind Field Modules of CALMET

- Slope Flows
- Kinematic Terrain Effects
- Terrain Blocking Effects
- Divergence Minimization
- Produces Gridded Fields of U, V, W Wind Components
- Inputs Include Domain-Scale Winds, Observations, and (optionally) Coarse-Grid Prognostic Model Winds
- Lambert Conformal Projection Capability

Prognostic Wind Field Model (CSUMM)

- Hydrostatic Primitive Equation (PE) Model
- Flows Generated in Response to Differential Surface
- Heating and Complex Terrain
- Land-Sea Breeze Circulations
- Slope-Valley Winds
- Produces Gridded Fields of U, V, W Wind Components, and other Meteorological Variables

(2) Receptor Modeling

Receptor models are generally contrasted with dispersion models which use estimates of pollutant emissions rates, meteorological transport, and chemical transformation mechanisms to estimate the contribution of each source to receptor concentrations. The two types of models are complementary, with each type having strengths which compensate for the weaknesses of the other. Receptor models use the chemical and physical characteristics of gases and particles measured at source and receptor to both identify the presence of and to quantify source contributions to receptor concentrations.

The modeling techniques include relatively simple techniques such as the use of "tracers of opportunity" such as lead (Pb), an indicator of mobile source contributions, and fluoride (F^-), an indicator of aluminum smelting. More complex multivariate statistical such as factor analysis and principal component analysis can be applied for relatively large and detailed databases (e.g., 50 or more samples with several dozen chemical parameters) with quite limited knowledge of emission source characteristics. The most robust methods are based on the use of multivariate statistical methods that attempt to "fit" known emission source profiles to observed SPM composition.

The most widely used of these is the Chemical Mass Balance model (CMB). Because of the limited number of samples and chemical constituents collected during 1998 and the limited number of source profiles only the CMB approach with observed concentrations and standard source profiles (e.g., those used or developed in previous receptor modeling studies) is used in the Study (Ref. 5-4).
The information required by and produced by the CMB model is shown in Figure 5.1.

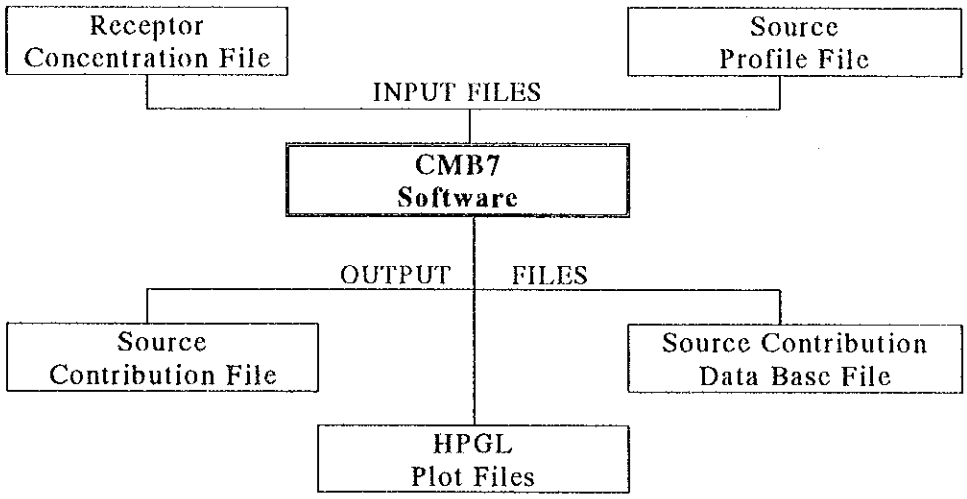

Figure 5.1 CMB7 Model Input and Output

The CMB consists of the following set of equations:

$$C_i = F_{i1}S_1 + F_{i2}S_2 + \ldots + F_{ij}S_j \ldots + F_{iJ}S_J \qquad i=1..I,\ j=1..J$$

where,

C_i: Concentration of species i measured at a receptor site

F_{ij}: Fraction of species i in emissions from source j

S_j: Estimate of the contribution of source j

I: Number of chemical species

J: Number of source types

5.1.3 Modeling Domain for Dispersion Models

The modeling domain is superimposed on a map of Macedonia as shown in Figure 5.2. The domain is a rectangular grid 60 km in the east-west direction and 40 km in the north-south direction. The four corners of the modeling domain are specified in the Gauss-Krieger coordinate system.

The modeling domain of 2400 km^2 covers all of Greater Skopje and also includes a small area of Serbia just to the northwest of Skopje.

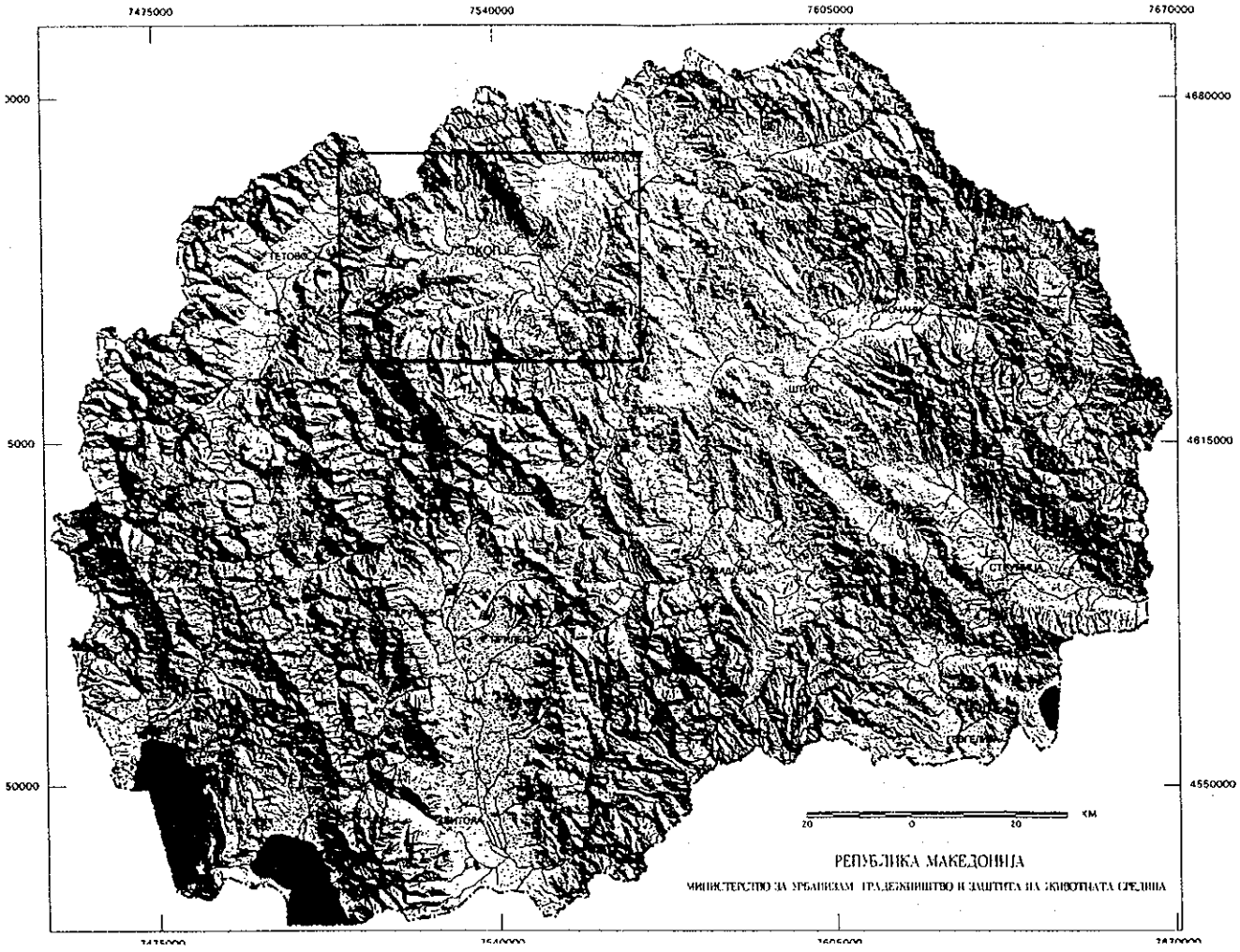

Figure 5.2 Location of the Modeling Domain for Skopje, Macedonia (Gauss-Krieger Coordinate System) 60 km x 40 km

5.2 Long-term Dispersion Model (ISC3LT)

5.2.1 Modeling Inputs

(1) Input Data

US-EPA ISC3LT (version 96113) was run in long-term mode (to determine annual average). The model was run with four seasonal modes to account for variations in seasonal temperatures and mixing heights. Emission source strength changes were model for two seasons (October 1 to March 31 - heating season) and (April 1 to September 30 - non-heating season) to reflect the strong seasonal change in emissions from the heating plants.

To perform long-term dispersion modeling, a complete year of hourly meteorological data is needed in order to prepare a joint frequency distribution of wind speed and direction by stability class. The complete meteorological data set includes measurements of hourly stability classification, vertical temperature gradient, wind speed and direction. The most complete data available for the Study was for calendar year 1996. To determine daytime atmospheric stability, solar insolation data is needed in conjunction with wind speed to determine stability. The methodology used to prepare the stability classification is discussed in the next section.

1) Stability Classification

The MHK Zletovo Metallurgical and Chemical Company collect the most complete data set of hourly solar radiation in Veles. To determine if the Veles site could reasonably be used in place of data from Skopje an assessment was performed. Correlation between the Veles solar radiation data and the limited solar radiation data collected by the RHI show relatively good correlation.
Figure 5.3 shows a comparison between the hourly averaged solar radiation data from Skopje and from Veles (Bolnica site) for two week time periods in January, March and May 1996 when a relatively complete set of observations were available at the Skopje site.

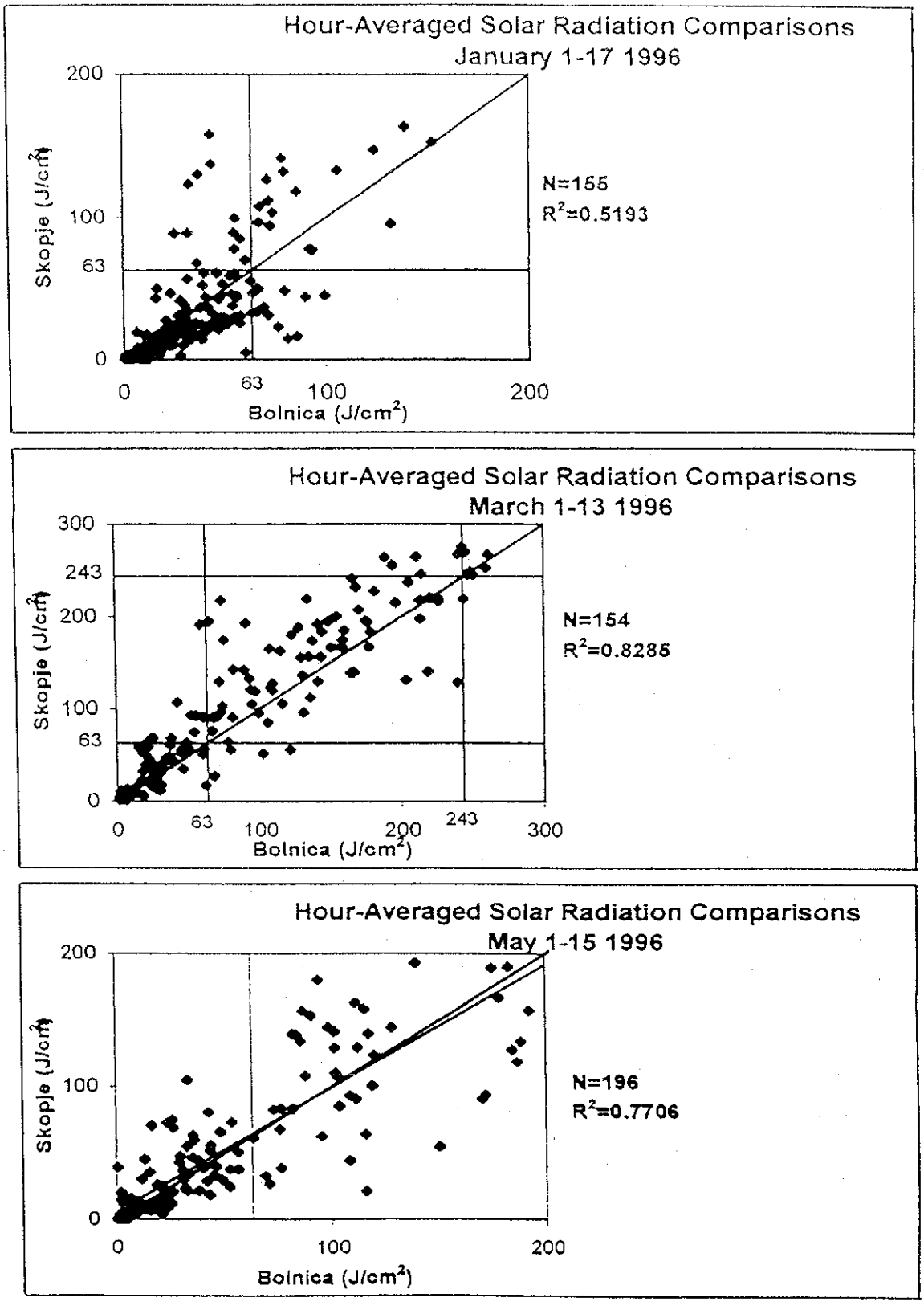

Figure 5.3 Intercomparison of Bolnica and Hydrometeorological Institute Solar Radiation Measurements for January, March and May 1996

In addition, no hourly solar radiation data was available from Veles after October 15. Because of the low solar elevation angle during this time daytime hours were assumed to be weakly unstable (stability class C), however wind speed adjustments to stability was included. Because no measure of vertical temperature gradient is available and hourly nighttime cloud cover data is only partially available cloud cover was conservatively assumed clear at night. This somewhat biases nighttime hours to slightly greater frequency of E (moderate stability) and F (strong stability) stability's, however wind speed adjustments to stability is included.

2) Wind Data

Hourly wind speed and direction from the 10 m above ground level the RHI anemometer from 1996 was used to prepare climatological average wind flow patterns. Plots of annual wind rose (the annual average prevailing wind direction as northwest to west in approximate orientation to the River Vardar and along the axis of the Skopje Valley) and two seasonal wind roses are shown in Figures D5.1 to D5.3 in Data Book. The prevailing wind directions during the October to March heating season (Figure D5.2) and non-heating season (Figure D5.3) are similar except that during the heating season calm conditions (wind speed < 1 m/s) occur almost twice as frequently.

3) Joint Frequency Distribution

A joint frequency distribution was prepared using the one year of complete meteorological data from 1996 using hourly wind data from the RHI and associated stability class. Four sets of joint frequency distributions were prepared, one for each season. Each joint frequency distribution consists of six matrices one for each stability class. Each matrix contains has 96 entries, 16 rows of wind directions (the standard 16 compass wind directions) by 6 columns of wind speeds categories. The model uses standard values for the median wind speed within each wind speed category. The standard values are; 1.50, 2.50, 4.30, 6.80, 9.50, and 12.50 m/s.

4) Temperatures

Seasonal average temperatures for each stability class were used as input to the model. The average daily maximum temperature was applied to stability classes A, B and C, the average daily minimum temperature to stability classes E and F, and the average daily temperature to stability class D. Values used are based on the ten-year record (1987-1996) from the RHI. Values are shown in Table 5.4.

Table 5.4 Seasonal Temperatures by Stability Class for ISC3LT

(Unit: °C)

Season	Stability Class					
	A	B	C	D	E	F
Winter (Jan-Mar)	8.6	8.6	8.6	3.9	-0.5	-0.5
Spring (Apr-Jun)	23.3	23.3	23.3	17.0	10.5	10.5
Summer (Jul-Sept)	29.8	29.8	29.8	22.6	15.6	15.6
Fall (Oct-Dec)	11.8	11.8	11.8	7.2	3.3	3.3

5) Mixing Heights

The upper-air sounding data for Skopje is only made once per day at 01:00 a.m. local standard time. The ISC3LT model needs at a minimum specification of the afternoon mixing height (near the time of maximum mixing height) and the morning mixing height (near the time of the minimum mixing height). No historical data are available for these measurements in Skopje and the nearest upper-air site is more than 500 km away and not representative of Skopje. Therefore, a site in the United States with similar meteorological and topographical setting was identified as a surrogate for Skopje. Based on a review of local climatology the city identified with the most similarities in climate and topographical setting was Boise, Idaho (Ref. 5-5). Seasonal mixing heights are shown in Table 5.5.

Table 5.5 Mean Mixing Heights by Season for Boise, Idaho and Used as Surrogate Mixing Heights for Skopje, Macedonia (Holzworth, 1972)

Season / Time	Winter (m)	Spring (m)	Summer (m)	Fall (m)
Morning	407	424	193	279
Afternoon	754	2329	2540	1409

As the common practice for urban areas, the mean afternoon mixing height will be applied for stability classes B and C, 1.5 times the mean afternoon mixing height to stability class A, and the average of the mean morning and afternoon mixing heights to stability class D.

6) Terrain Inputs

The ISCLT model does not need gridded terrain inputs when the dry deposition option

is not used. Relative release heights above local terrain height are specified on input for each emission source location.

7) Emission Inputs

All sources are modeled as point or area sources. Emission rates are modeled using annual average emission rate estimate for 1996. Seasonal adjustments are made for the heating plants facilities.

Annual average emission rates for major and medium size stationary sources were developed based on survey response answers from the Questionnaire on Stationary Source Emission Inventory as distributed by the Ministry of Environment (MOE). Emissions were adjusted for operating schedules as specified in the inventory. These ranged from 8-hour operations to 24-hour operating periods. Table 5.6 identifies the number of stacks modeled as point sources and the total annual average emission rates for chemical specie.

Table 5.6 Annual Average Emission Rates for Major and Medium Size Stationary Point Sources Used in the ISC3LT Modeling

Pollutant	Number of Point Sources Modeled	Annual Average Emission Rate (g/s)
SO_2	68	625
NO_2	71	173
SPM	68	17.4
CO	68	226

Other emission source types such as residential heating, mobile sources, small combustion sources (< 200 kg/h fuel combustion rate) and construction activity were modeled as area sources. Data for school heating and administrative buildings were modeled as area sources and were summed within a grid cell to yield a total annual average flux emission rate (g/m^2-s). The configuration for each area source was a square, 500 x 500 m, oriented north-south and east-west within the local Gauss-Krieger coordinate system. Input location was specified in local Gauss-Krieger coordinate system specifying the southwest corner as the location, release height in meters, and the annual average flux emission rate in g/m^2-s. Separate files were created for each pollutant type. Other area emission sources were unavailable at the present time and emission rates were estimated based on per capita emission factors from emission inventories for countries near Macedonia, supplemented by US emission ratios (as European data did not have SPM emissions). The information used to estimate these emissions was the CORINAIR94 emission inventory from Greece,

Croatia, Austria and Italy and CORINAIR90 emissions for the same four countries plus Slovenia and Bulgaria. No SPM emissions were available in either inventory so the ratio of PM_{10} relative to CO, NOx and SO_2 from US EPA95 trends report emission totals was used to estimate the SPM. These per capita emissions included all source types of emissions (industrial, mobile, area) so based on the estimated CO emissions from mobile sources (Republic of Macedonia, 1996) the emissions were adjusted so that CO emissions from mobile sources accounted for approximately 65% of the CO emissions for Skopje. This is fairly typical of the mobile source CO contribution for industrialized urban areas. This adjustment was extended to all pollutants. These area source pollutants were assumed to be 75% emitted during the daytime and 25% and night. Table 5.7 shows the annual average emission density for each area source air pollutant as modeled. Table 5.8 shows the total annual average emissions for each pollutant by major source categories. Mobile source fraction is from the Macedonia National Environmental Action Plan (Ref. 2-5).

Table 5.7 Annual Average Emission Density for Area Sources in Skopje, Macedonia as Used in the ISC3LT Modeling

Pollutant	Emission Density ($gm/s\text{-}km^2$)
SO_2	6.84
NO_2	5.13
CO	20.5
SPM	10.3

Table 5.8 Annual Average Emissions and Distribution by Major Source Categories for Four Air Pollution in Skopje, Macedonia

Source Type	SO_2 t/yr (%)	NO_2 t/yr (%)	CO t/yr (%)	SPM t/yr (%)
Heating Plants	5,840 (22.5)	1,460 (14.3)	548 (2.1)	182 (1.8)
Combustion Sources	13,370 (53.5)	4,015 (39.3)	6,570 (25.2)	365 (3.7)
Mobile Sources	88.6 (0.4)	2,600 (25.5)	16,400 (62.8)	410* (4.1)
Area Sources	6,116 (23.6)	2,130 (20.9)	2,580 (9.9)	9,080 (90.4)
Total	25,915 (100)	10,205 (100)	26,098 (100)	10,037 (100)

8) Other Modeling Options

No wet or dry deposition - No information on particle size, density and mass fraction is available. Hence we will conservatively assume no deposition. This is reasonable for the near field concentrations, particularly if particles are 10 microns or less.

- Use urban dispersion curves – Skopje is a city with many tall structures which act to enhance atmospheric dispersion
- Use final plume rise, stack-tip downwash, buoyancy-induced dispersion
- Use default wind speed profile exponents; and
- Use urban vertical potential temperature gradients
- No building downwash
- Decay-half life (4-hours for SO_2)

(2) Receptor Placement

Receptors were placed in a uniform Cartesian gridded array covering the entire modeling domain at 1,000 m horizontal resolution. Discrete receptors were placed at the nine RHI and seven IPH existing measuring points. The local Gauss-Krieger coordinates were determined from location maps provided by the Macedonian side.

5.2.2 Output Results and Model Verification

(1) Air Quality Data for Model Verification - Present Air Quality

1) Model Verification

Modeling results are compared with the annual average monitored results for SO_2 and SPM using data converted from Black Smoke (BS) to SPM for the 1996. Comparisons between modeled and observed are shown for each measurement point for SO_2 and SPM in Tables D5.1 and D5.2 in Data Book. For SO_2 all points show an overprediction ranging from approximately a factor of 2 to 4. The cause for this overprediction is most likely a result of overestimating SO_2 emissions. In the Study reported annual average operating emissions were used to model SO_2 concentrations within Greater Skopje, but these emission estimates are based on the operating capacity rather than being adjusted for actual annual operating rates which may be considerably lower, therefore it is not surprising that the model overpredicts observed concentrations. Also, area source emissions are only approximated, the uncertainty associated with these emissions is very large. For SPM the model did very well for

simulating the annual average concentration for monitors located in and around the city center (AMSM, Karpos IV, and University – Library Center), showing an annual average concentration of around 45 $\mu g/m^3$. For the measurement points located outside the city center the model overpredicted concentrations by factors of 1.5 to 4. The four recently installed continuous monitoring stations (which include two stations outside the city center) by the Study show monthly average concentrations at approximately the same level as those modeled, ranging from 44 to 72 $\mu g/m^3$ for April to June. The BS measurement, in principle, is lower than the mass method, such as SPM. The difference between the values predicted and observed is examined from the survey results. According to the results from questionnaire and visiting research, the average operation rate of factories is presently 30 to 40% of the maximum working. Emissions with maximum working were used for modeling input, therefore the overestimation of SO_2 emissions was found to be clear. Moreover, according to the results from comparison of measurement values for SPM and BS, which is obtained in the Study, it was proved that the values of BS showed only about a half of that of SPM. Therefore, it is understandable that the values predicted and observed will approximate much more with consideration on the facts above.
Figures 5.4 to 5.7 show the spatial distribution within the modeling domain of annual average SO_2, SPM, NO_2 and CO.

a) SO_2 Dispersion

For SO_2 the concentration pattern is consistent with patterns developed from monitored data (Republic of Macedonia, 1996) with the exception of the two highest concentrations; i) the highest simulated concentration located near Zelezara, Valavnica which is dominated by emissions from the Clinc Center at Vodnjanska 17 and, ii) the second highest simulated concentration located near n. Lisice ul. Mihail Glinka 4, prof. Durnev which is dominated by emissions from OHIS Prvomajska bb (chemical plant). Further investigation is needed to verify the plants stack parameters and actual annual average operating emissions.

b) SPM Dispersion

For SPM the concentration pattern is very similar to the pattern developed from monitored data (Republic of Macedonia, 1996) although the spatial area exceeding 40 $\mu g/m^3$ is larger for the modeled concentration.

c) NO_2 Dispersion

Figure 5.6 shows the spatial concentration pattern for NO_2 that is consistent with four recently installed continuous NO_2 monitors (Gazi Baba, Center, Karps, Lisice) which show a monthly average range of 9 to 45 $\mu g/m^3$ for the three months from April to June 1998.

d) CO Dispersion

Figure 5.7, which shows the annual average concentration for CO, appears to be well below observed concentration levels. This is probably reflective of a severe underestimation in the CO mobile source emission inventory and not including any ambient background concentration.

2) Source Contribution

Table 5.9 shows the source contribution by source type for the discrete receptor locations (16 measurement points) for each pollutant source type. For SO_2, source contributions appear to have a wide variation with some points dominated by combustion sources while others are primarily influenced by area sources. Modeled NOx source contributions are predominately from area sources emissions with the exception of the cement factory. CO and SPM source contributions are both dominated by area source emissions.

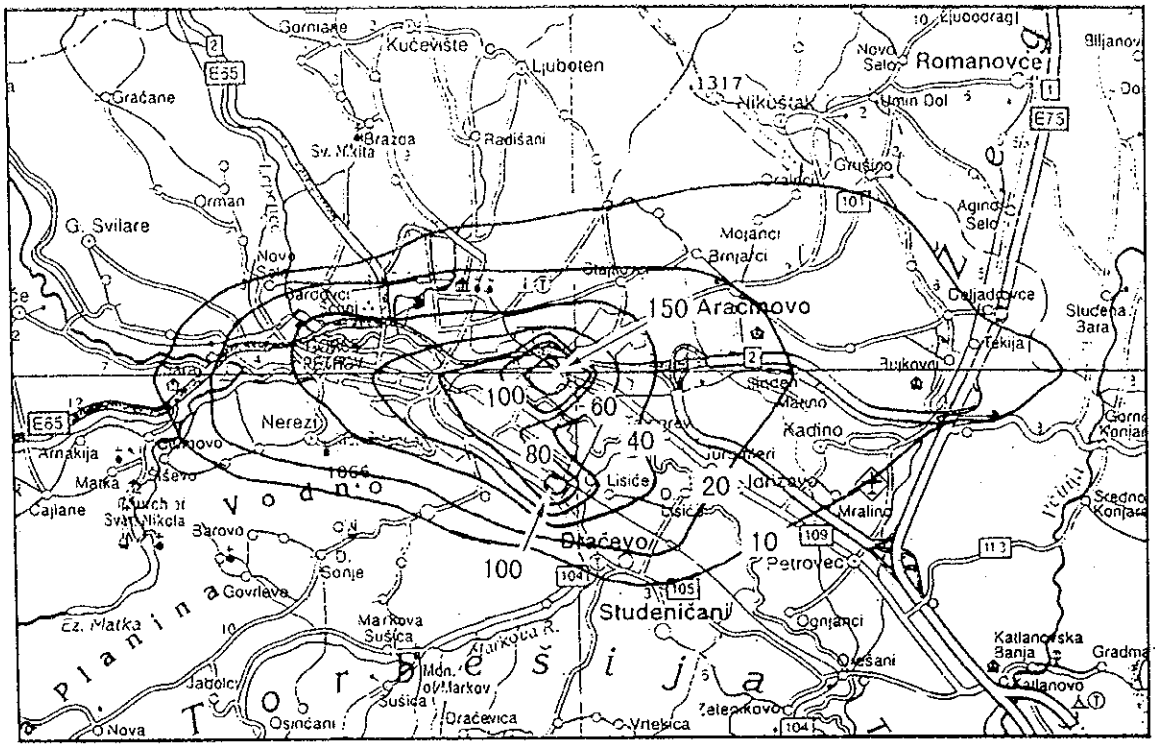

Figure 5.4 ISC3LT 1996 Annual Average SO_2 Concentration ($\mu g/m^3$)

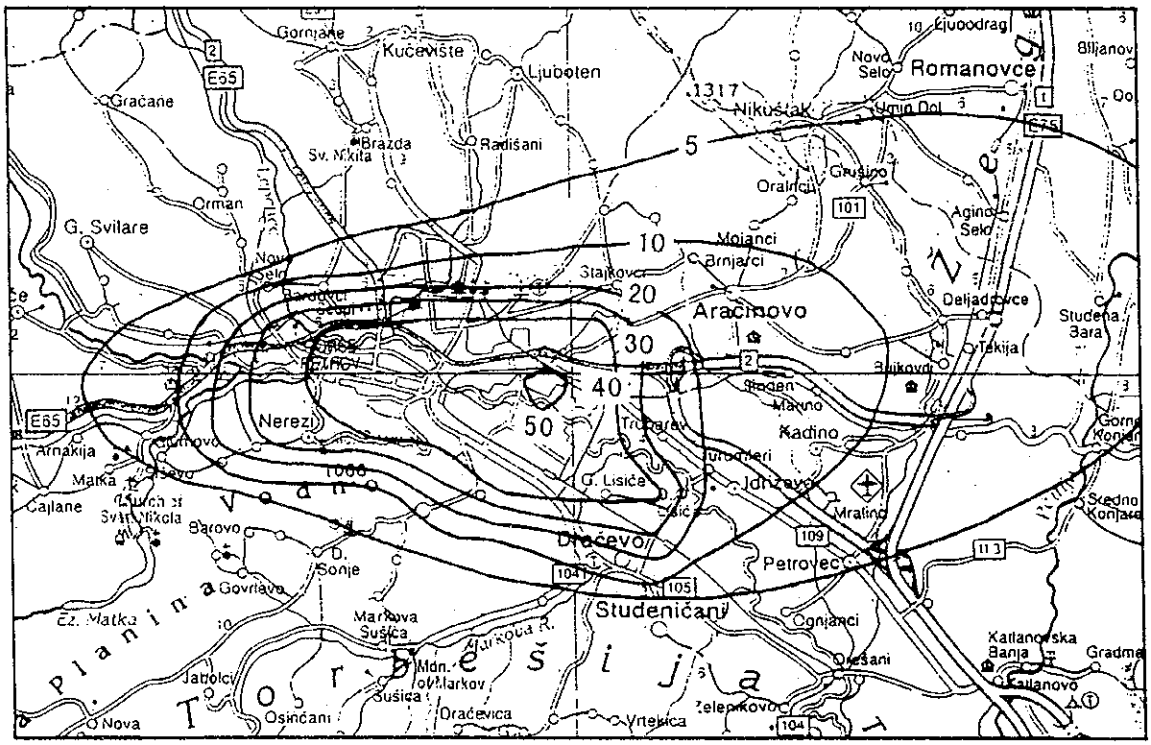

Figure 5.5 ISC3LT 1996 Annual Average SPM Concentration ($\mu g/m^3$)

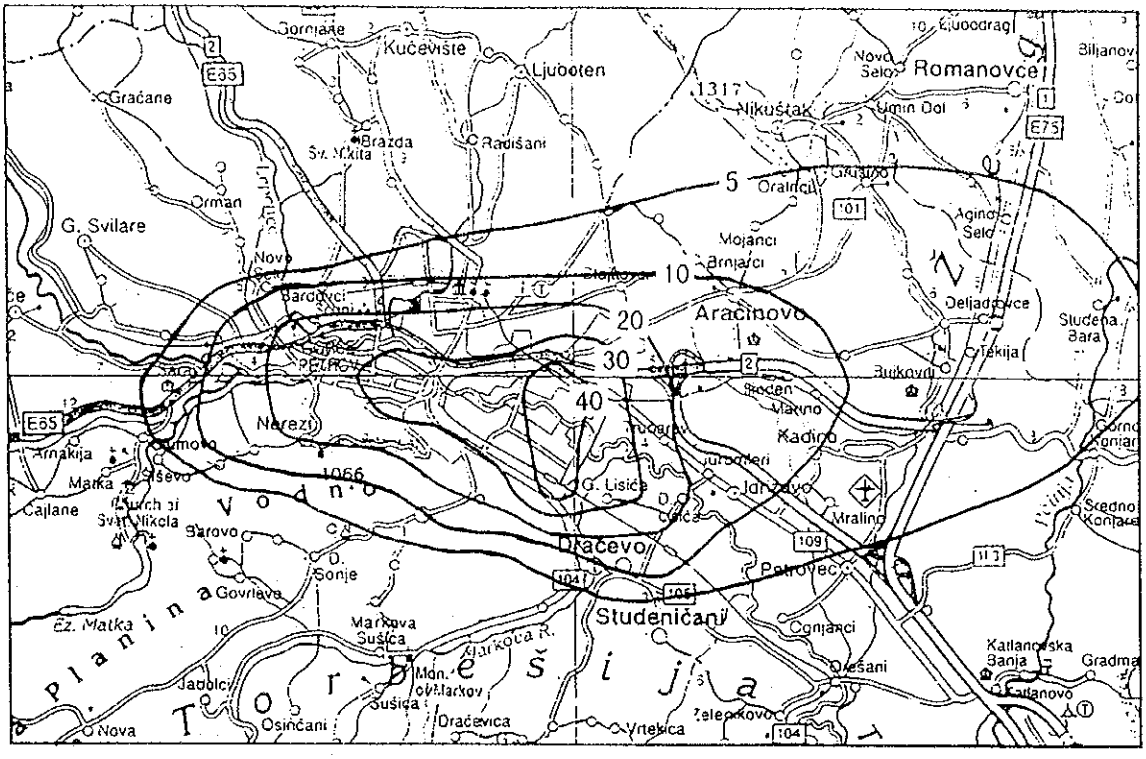

Figure 5.6 ISC3LT 1996 Annual Average NO_2 Concentration ($\mu g/m^3$)

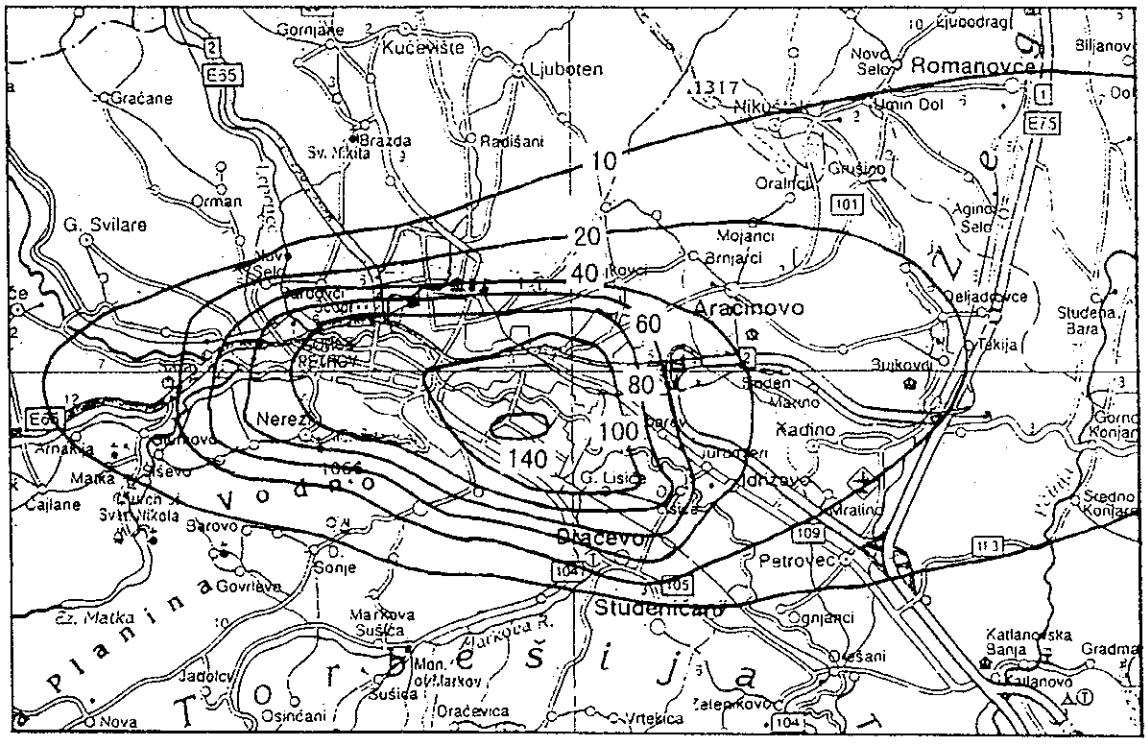

Figure 5.7 ISC3LT 1996 Annual Average CO Concentration ($\mu g/m^3$)

Table 5.9 (1) Source Contributions of 1996 Annual Average Concentrations at the Discrete Receptor Locations

Receptor Name	UTM X	UTM Y	Concentration (in µg/m³) Heating Plants	Combustion Sources	Area Sources	Percent of Total Concentration Heating Plants	Combustion Sources	Area Sources
SO_2								
RHI Points								
AMSM	535.18	4650.15	10.49	22.47	28.98	16.9%	36.3%	46.8%
Fruit Farming Institute - K. Voda	537.45	4648.25	2.87	25.39	28.60	5.0%	44.7%	50.3%
HMI – Karpos	533.65	4652.60	3.52	10.51	26.78	8.6%	25.8%	65.6%
Dracevo - K. Voda	541.50	4647.00	2.50	31.81	37.98	3.5%	44.0%	52.5%
Avtokomanda - G. Baba	538.80	4651.00	7.01	47.71	30.02	8.3%	56.3%	35.4%
Karpos IV - Karpos	532.80	4651.25	5.65	9.40	27.25	13.4%	22.2%	64.4%
University Lib - Center	536.85	4650.55	8.91	50.00	29.59	10.1%	56.5%	33.4%
J. B. Tito	535.90	4650.20	10.87	49.55	29.29	12.1%	55.2%	32.7%
Novo Lisice	539.60	4648.85	6.53	31.77	29.76	9.6%	46.7%	43.7%
IPH Points								
Pivara	538.40	4650.10	3.31	57.16	29.82	3.7%	63.3%	33.0%
Jane Sandanski (Kinder Galten)	538.70	4649.25	6.93	43.17	29.37	8.7%	54.3%	37.0%
Cement Factory	538.30	4647.40	1.29	17.10	38.52	2.3%	30.1%	67.7%
Hotel Panorama (Recreation Zone)	535.40	4648.95	4.20	5.68	27.63	11.2%	15.1%	73.6%
Elementary School Dimo Hadzi Dimov	531.50	4651.35	7.11	9.84	25.70	16.7%	23.1%	60.3%
DDD Station	537.50	4652.75	6.09	10.08	27.47	14.0%	23.1%	62.9%
Municipal Health Institute	536.85	4649.30	3.53	95.68	28.60	2.8%	74.9%	22.4%
NO_x								
RHI Points								
AMSM	535.18	4650.15	2.70	6.24	23.08	8.4%	19.5%	72.1%
Fruit Farming Institute - K. Voda	537.45	4648.25	0.76	6.40	22.70	2.6%	21.4%	76.0%
HMI – Karpos	533.65	4652.60	0.88	2.22	21.21	3.6%	9.1%	87.2%
Dracevo - K. Voda	541.50	4647.00	0.73	18.74	30.17	1.5%	37.8%	60.8%
Avtokomanda - G. Baba	538.80	4651.00	1.85	6.14	24.10	5.8%	19.1%	75.1%
Karpos IV - Karpos	532.80	4651.25	1.46	2.15	21.60	5.8%	8.5%	85.7%
University Lib - Center	536.85	4650.55	2.27	6.07	23.63	7.1%	19.0%	73.9%
J. B. Tito	535.90	4650.20	2.82	7.10	23.38	8.5%	21.3%	70.2%
Novo Lisice	539.60	4648.85	1.84	8.93	23.79	5.3%	25.8%	68.8%
IPH Points								
Pivara	538.40	4650.10	0.82	7.09	23.86	2.6%	22.3%	75.1%
Jane Sandanski (Kinder Galten)	538.70	4649.25	1.91	5.42	23.46	6.2%	17.6%	76.2%
Cement Factory	538.30	4647.40	0.33	50.28	30.34	0.4%	62.1%	37.5%
Hotel Panorama (Recreation Zone)	535.40	4648.95	1.09	3.52	21.96	4.1%	13.3%	82.6%
Elementary School Dimo Hadzi Dimov	531.50	4651.35	1.75	2.06	20.32	7.2%	8.5%	84.2%
DDD Station	537.50	4652.75	1.47	1.84	22.02	5.8%	7.3%	86.9%
Municipal Health Institute	536.85	4649.30	0.92	6.08	22.77	3.1%	20.4%	76.5%

Table 5.9 (2) Source Contributions of 1996 Annual Average Concentrations at the Discrete Receptor Locations

Receptor Name	UTM X	UTM Y	Concentration (in μg/m³) Heating Plants	Combustion Sources	Area Sources	Percent of Total Concentration Heating Plants	Combustion Sources	Area Sources
CO								
RHI Points								
AMSM	535.18	4650.15	0.97	5.27	91.76	1.0%	5.4%	93.6%
Fruit Farming Institute - K. Voda	537.45	4648.25	0.29	20.70	90.14	0.3%	18.6%	81.1%
HMI – Karpos	533.65	4652.60	0.30	1.79	84.34	0.3%	2.1%	97.6%
Dracevo - K. Voda	541.50	4647.00	0.30	37.19	119.13	0.2%	23.7%	76.1%
Avtokomanda - G. Baba	538.80	4651.00	0.69	8.46	95.84	0.7%	8.1%	91.3%
Karpos IV - Karpos	532.80	4651.25	0.55	2.50	85.90	0.6%	2.8%	96.6%
University Lib - Center	536.85	4650.55	0.81	8.35	93.97	0.8%	8.1%	91.1%
J. B. Tito	535.90	4650.20	1.05	8.21	92.96	1.0%	8.0%	90.9%
Novo Lisice	539.60	4648.85	0.75	28.01	94.51	0.6%	22.7%	76.7%
IPH Points								
Pivara	538.40	4650.10	0.26	36.15	94.88	0.2%	27.5%	72.3%
Jane Sandanski (Kinder Galten)	538.70	4649.25	0.77	9.50	93.25	0.7%	9.2%	90.1%
Cement Factory	538.30	4647.40	0.12	115.33	119.96	0.0%	49.0%	51.0%
Hotel Panorama (Recreation Zone)	535.40	4648.95	0.39	5.46	87.28	0.4%	5.9%	93.7%
Elementary School Dimo Hadzi Dimov	531.50	4651.35	0.58	2.30	80.81	0.7%	2.7%	96.6%
DDD Station	537.50	4652.75	0.46	2.67	87.55	0.5%	2.9%	96.5%
Municipal Health Institute	536.85	4649.30	0.34	14.09	90.52	0.3%	13.4%	86.2%
SPM								
RHI Points								
AMSM	535.18	4650.15	0.54	0.34	45.97	1.2%	0.7%	98.1%
Fruit Farming Institute - K. Voda	537.45	4648.25	0.13	0.63	45.16	0.3%	1.4%	98.3%
HMI – Karpos	533.65	4652.60	0.22	0.63	42.25	0.5%	1.5%	98.0%
Dracevo - K. Voda	541.50	4647.00	0.08	1.25	59.68	0.1%	2.0%	97.8%
Avtokomanda - G. Baba	538.80	4651.00	0.37	1.18	48.01	0.7%	2.4%	96.9%
Karpos IV - Karpos	532.80	4651.25	0.30	0.39	43.03	0.7%	0.9%	98.4%
University Lib - Center	536.85	4650.55	0.50	0.37	47.08	1.0%	0.8%	98.2%
J. B. Tito	535.90	4650.20	0.54	0.35	46.57	1.1%	0.7%	98.1%
Novo Lisice	539.60	4648.85	0.21	0.93	47.35	0.4%	1.9%	97.7%
IPH Points								
Pivara	538.40	4650.10	0.25	0.75	47.53	0.5%	1.5%	97.9%
Jane Sandanski (Kinder Galten)	538.70	4649.25	0.24	0.75	46.71	0.5%	1.6%	97.9%
Cement Factory	538.30	4647.40	0.08	2.95	60.10	0.1%	4.7%	95.2%
Hotel Panorama (Recreation Zone)	535.40	4648.95	0.22	0.31	43.73	0.5%	0.7%	98.8%
Elementary School Dimo Hadzi Dimov	531.50	4651.35	0.47	0.33	40.49	1.1%	0.8%	98.1%
DDD Station	537.50	4652.75	0.49	0.99	43.86	1.1%	2.2%	96.7%
Municipal Health Institute	536.85	4649.30	0.18	0.36	45.35	0.4%	0.8%	98.8%

(2) Future Year and Emission Control Strategy Modeling Results – ISC3LT

1) Future Scenario

Model inputs for the future year simulation are identical to base year modeling effort with the exception of changes to the emission inputs. For the future year (2008) each stationary point source was increased by 20% to reflect additional industrial growth, while area sources remained constant. The control strategy was to switch from oil to natural gas for all of Skopje heating plants. Emissions from the heating facilities were reduced by 80% under this control scenario.

2) Modeling Results

Figures 5.8 to 5.11 show the annual average spatial distribution of SO_2, SPM, NO_2 and CO with the implementation of the control strategy. For all pollutants, including SO_2, the change in emissions resulted in little change to the annual average concentrations. This is because the heating plants contribute little to the overall SPM, NO_2, and CO emissions (Table 5.10).
Additionally, these sources only operate for half the year and are emitted from relatively tall stacks. This enables pollutants to be widely distributed.

3) Source Contribution

Table 5.10 shows the source contribution by source type for the monitoring locations for each pollutant source type for the future year with the control strategy. As shown in Table 5.10 the source contribution from the heating facilities for SO_2 is much smaller in 2008 than for 1996 with the control strategy implemented, however the 20% growth for other combustion sources erodes the benefit of the control strategy, with a net result of little change in the modeled SO_2 concentration. Conversion of fuel from the heavy oil to low sulfur fuel at other combustion sources is therefore needed.

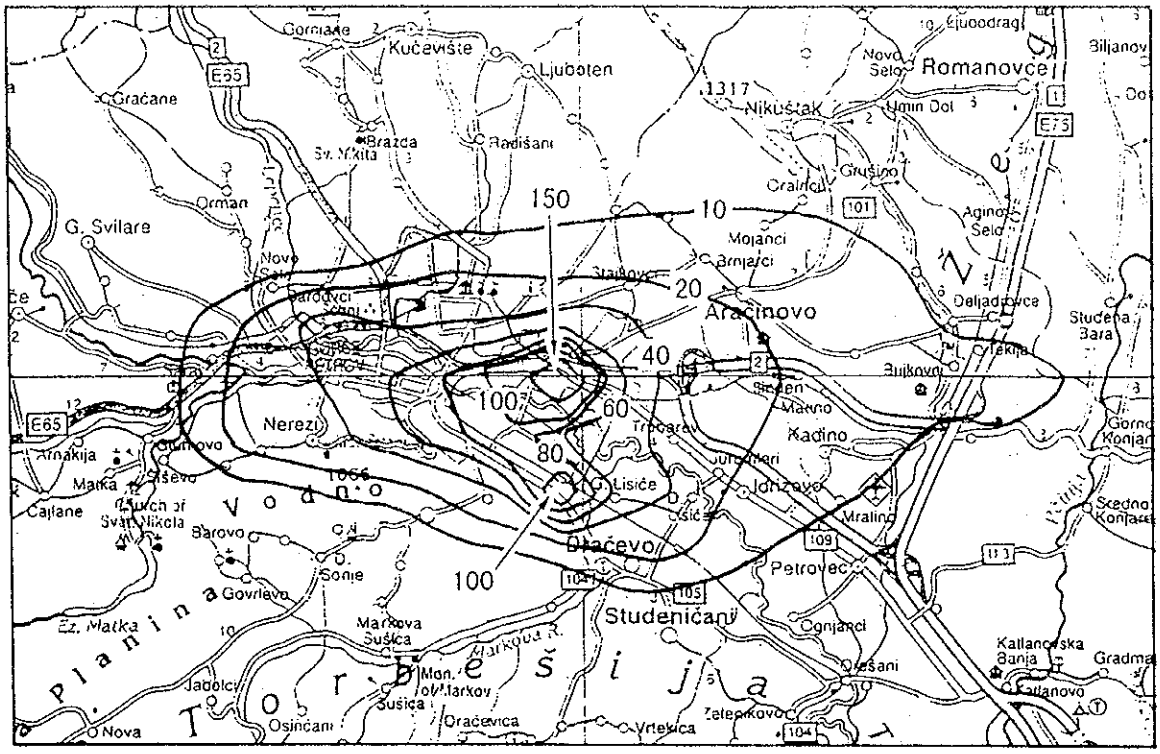

Figure 5.8 ISC3LT Annual Average SO_2 Concentration ($\mu g/m^3$) for 2008 with Control for Skopje

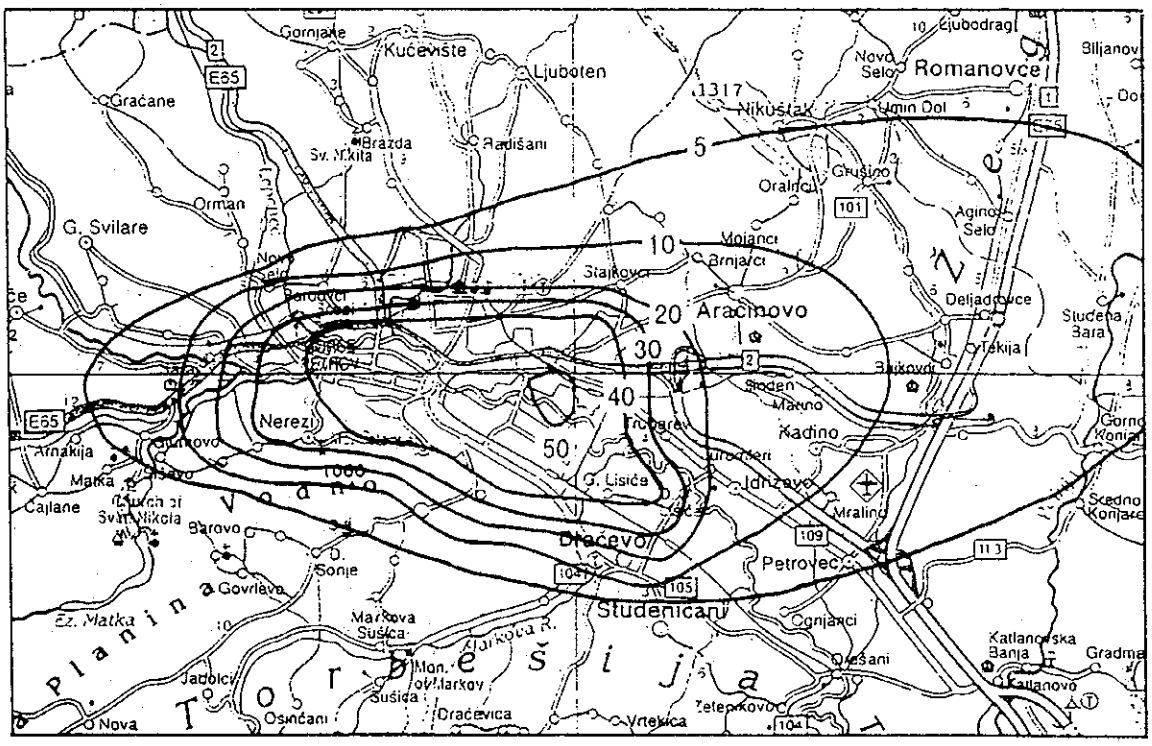

Figure 5.9 ISC3LT Annual Average SPM Concentration ($\mu g/m^3$) for 2008 with Control for Skopje

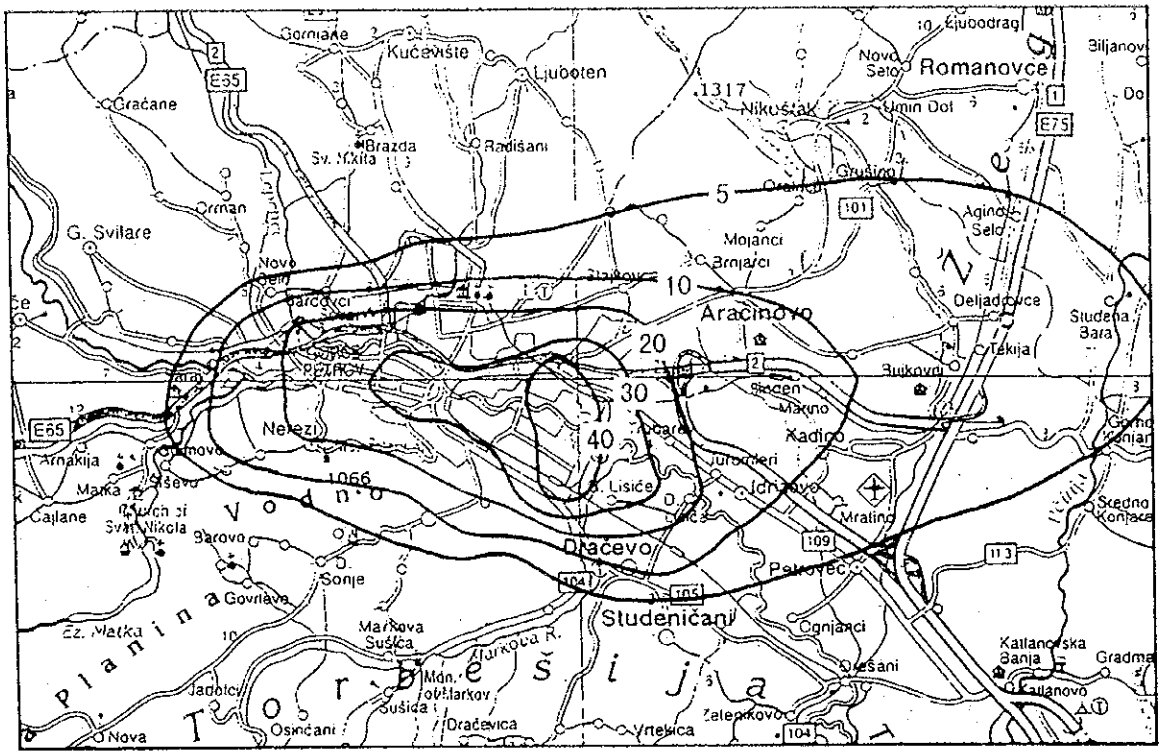

Figure 5.10 ISC3LT Annual Average NO_2 Concentration ($\mu g/m^3$) for 2008 with Control for Skopje

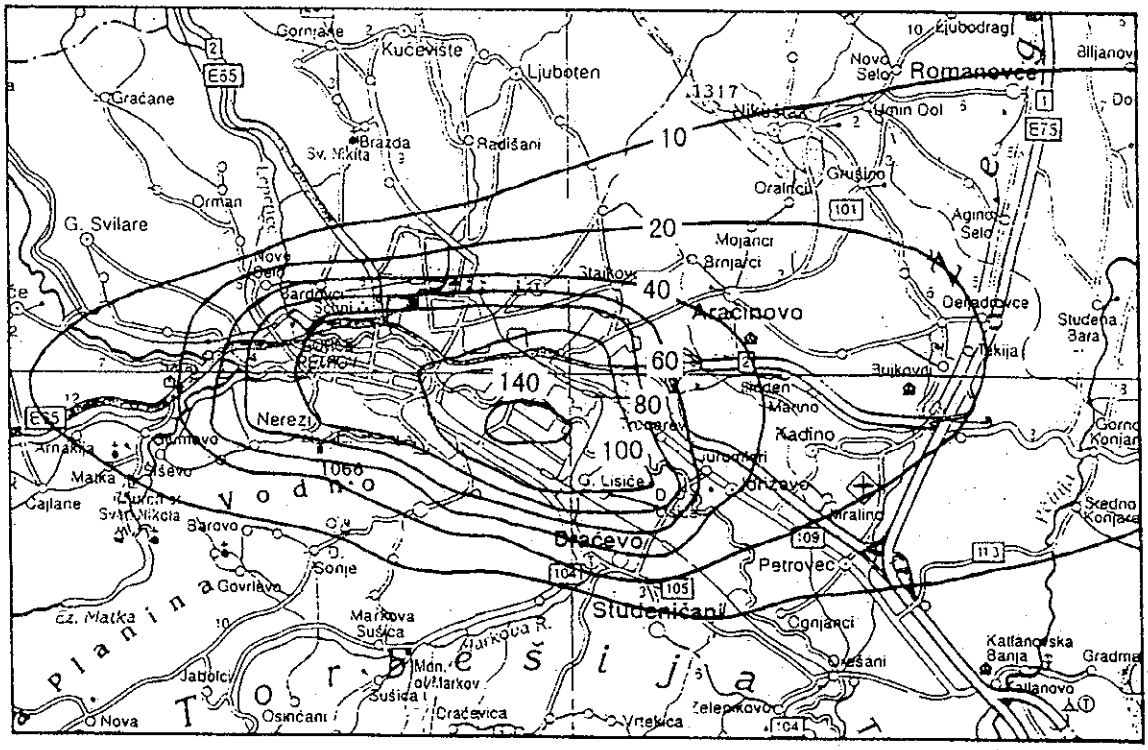

Figure 5.11 ISC3LT Annual Average CO Concentration ($\mu g/m^3$) for 2008 with Control for Skopje

Table 5.10 (1) Source Contributions of 2008 Annual Average Concentrations at the Discrete Receptor Locations

Receptor Name	UTM X	UTM Y	Concentration (in µg/m3) Heating Plants	Combustion Sources	Area Sources	Percent of Total Concentration Heating Plants	Combustion Sources	Area Sources
SO_2								
RHI Points								
AMSM	535.18	4650.15	2.10	26.96	28.98	3.6%	46.4%	49.9%
Fruit Farming Institute - K. Voda	537.45	4648.25	0.57	30.47	28.60	1.0%	51.1%	48.0%
HMI – Karpos	533.65	4652.60	0.70	12.61	26.78	1.8%	31.5%	66.8%
Dracevo - K. Voda	541.50	4647.00	0.50	38.17	37.98	0.7%	49.8%	49.6%
Avtokomanda - G. Baba	538.80	4651.00	1.40	57.25	30.02	1.6%	64.6%	33.9%
Karpos IV - Karpos	532.80	4651.25	1.13	11.28	27.25	2.9%	28.4%	68.7%
University Lib - Center	536.85	4650.55	1.78	60.00	29.59	2.0%	65.7%	32.4%
J. B. Tito	535.90	4650.20	2.17	59.46	29.29	2.4%	65.4%	32.2%
Novo Lisice	539.60	4648.85	1.31	38.13	29.76	1.9%	55.1%	43.0%
IPH Points								
Pivara	538.40	4650.10	0.66	68.59	29.82	0.7%	69.2%	30.1%
Jane Sandanski (Kinder Galten)	538.70	4649.25	1.39	51.80	29.37	1.7%	62.7%	35.6%
Cement Factory	538.30	4647.40	0.26	20.52	38.52	0.4%	34.6%	65.0%
Hotel Panorama (Recreation Zone)	535.40	4648.95	0.84	6.82	27.63	2.4%	19.3%	78.3%
Elementary School Dimo Hadzi Dimov	531.50	4651.35	1.42	11.80	25.70	3.7%	30.3%	66.0%
DDD Station	537.50	4652.75	1.22	12.10	27.47	3.0%	29.7%	67.4%
Municipal Health Institute	536.85	4649.30	0.71	114.81	28.60	0.5%	79.7%	19.8%
NO_2								
RHI Points								
AMSM	535.18	4650.15	0.54	7.49	23.08	1.7%	24.1%	74.2%
Fruit Farming Institute - K. Voda	537.45	4648.25	0.15	7.68	22.70	0.5%	25.2%	74.3%
HMI – Karpos	533.65	4652.60	0.18	2.67	21.21	0.7%	11.1%	88.2%
Dracevo - K. Voda	541.50	4647.00	0.15	22.49	30.17	0.3%	42.6%	57.1%
Avtokomanda - G. Baba	538.80	4651.00	0.37	7.37	24.10	1.2%	23.1%	75.7%
Karpos IV - Karpos	532.80	4651.25	0.29	2.58	21.60	1.2%	10.5%	88.3%
University Lib - Center	536.85	4650.55	0.45	7.28	23.63	1.4%	23.2%	75.3%
J. B. Tito	535.90	4650.20	0.56	8.52	23.38	1.7%	26.3%	72.0%
Novo Lisice	539.60	4648.85	0.37	10.71	23.79	1.1%	30.7%	68.2%
IPH Points								
Pivara	538.40	4650.10	0.16	8.51	23.86	0.5%	26.2%	73.3%
Jane Sandanski (Kinder Galten)	538.70	4649.25	0.38	6.51	23.46	1.3%	21.4%	77.3%
Cement Factory	538.30	4647.40	0.07	60.34	30.34	0.1%	66.5%	33.4%
Hotel Panorama (Recreation Zone)	535.40	4648.95	0.22	4.23	21.96	0.8%	16.0%	83.2%
Elementary School Dimo Hadzi Dimov	531.50	4651.35	0.35	2.47	20.32	1.5%	10.7%	87.8%
DDD Station	537.50	4652.75	0.29	2.21	22.02	1.2%	9.0%	89.8%
Municipal Health Institute	536.85	4649.30	0.18	7.29	22.77	0.6%	24.1%	75.3%

Table 5.10 (2) Source Contributions of 2008 Annual Average Concentrations at the Discrete Receptor Locations

Receptor Name	UTM X	UTM Y	Concentration (in µg/m3) Heating Plants	Combustion Sources	Area Sources	Percent of Total Concentration Heating Plants	Combustion Sources	Area Sources
CO								
RHI Points								
AMSM	535.18	4650.15	0.19	6.33	91.76	0.2%	6.4%	93.4%
Fruit Farming Institute - K. Voda	537.45	4648.25	0.06	24.84	90.14	0.1%	21.6%	78.4%
HMI – Karpos	533.65	4652.60	0.06	2.15	84.34	0.1%	2.5%	97.4%
Dracevo - K. Voda	541.50	4647.00	0.06	44.62	119.13	0.0%	27.2%	72.7%
Avtokomanda - G. Baba	538.80	4651.00	0.14	10.15	95.84	0.1%	9.6%	90.3%
Karpos IV - Karpos	532.80	4651.25	0.11	3.00	85.90	0.1%	3.4%	96.5%
University Lib - Center	536.85	4650.55	0.16	10.01	93.97	0.2%	9.6%	90.2%
J. B. Tito	535.90	4650.20	0.21	9.86	92.96	0.2%	9.6%	90.2%
Novo Lisice	539.60	4648.85	0.15	33.61	94.51	0.1%	26.2%	73.7%
IPH Points								
Pivara	538.40	4650.10	0.05	43.38	94.88	0.0%	31.4%	68.6%
Jane Sandanski (Kinder Galten)	538.70	4649.25	0.15	11.40	93.25	0.1%	10.9%	89.0%
Cement Factory	538.30	4647.40	0.02	138.39	119.96	0.0%	53.6%	46.4%
Hotel Panorama (Recreation Zone)	535.40	4648.95	0.08	6.55	87.28	0.1%	7.0%	92.9%
Elementary School Dimo Hadzi Dimov	531.50	4651.35	0.12	2.76	80.81	0.1%	3.3%	96.6%
DDD Station	537.50	4652.75	0.09	3.20	87.55	0.1%	3.5%	96.4%
Municipal Health Institute	536.85	4649.30	0.07	16.90	90.52	0.1%	15.7%	84.2%
SPM								
RHI Points								
AMSM	535.18	4650.15	0.11	0.41	45.97	0.2%	0.9%	98.9%
Fruit Farming Institute - K. Voda	537.45	4648.25	0.03	0.76	45.16	0.1%	1.6%	98.3%
HMI – Karpos	533.65	4652.60	0.04	0.75	42.25	0.1%	1.7%	98.2%
Dracevo - K. Voda	541.50	4647.00	0.02	1.49	59.68	0.0%	2.4%	97.5%
Avtokomanda - G. Baba	538.80	4651.00	0.07	1.41	48.01	0.1%	2.9%	97.0%
Karpos IV - Karpos	532.80	4651.25	0.06	0.47	43.03	0.1%	1.1%	98.8%
University Lib - Center	536.85	4650.55	0.10	0.45	47.08	0.2%	0.9%	98.8%
J. B. Tito	535.90	4650.20	0.11	0.42	46.57	0.2%	0.9%	98.9%
Novo Lisice	539.60	4648.85	0.04	1.11	47.35	0.1%	2.3%	97.6%
IPH Points								
Pivara	538.40	4650.10	0.05	0.89	47.53	0.1%	1.8%	98.1%
Jane Sandanski (Kinder Galten)	538.70	4649.25	0.05	0.90	46.71	0.1%	1.9%	98.0%
Cement Factory	538.30	4647.40	0.02	3.54	60.10	0.0%	5.6%	94.4%
Hotel Panorama (Recreation Zone)	535.40	4648.95	0.04	0.38	43.73	0.1%	0.9%	99.0%
Elementary School Dimo Hadzi Dimov	531.50	4651.35	0.09	0.39	40.49	0.2%	1.0%	98.8%
DDD Station	537.50	4652.75	0.10	1.18	43.86	0.2%	2.6%	97.2%
Municipal Health Institute	536.85	4649.30	0.04	0.43	45.35	0.1%	0.9%	99.0%

5.3 Short-term Dispersion Model (CALPUFF)

The CALPUFF modeling system was run in episodic mode to simulate hourly and daily average SO_2 concentration within 60x40 km modeling domain which encompasses all of Skopje. The time period for modeling was from 9:00 p.m. on January 13 to 0:00 a.m. on January 15, 1998. This time period was selected from three episodes where 24-hour SO_2 concentrations exceeded 50 $\mu g/m^3$ from the winter of 1997 and 1998; from December 11 to 13 (1997), from January 14 to 16 (1998), and from February 11 to 13 (1998). Hourly emission rates and meteorological data were input to the model on an hourly basis to reflect dynamic changes that occur during a typical episode. The CALPUFF modeling system is composed of two principal components; i) CALMET- a diagnostic meteorological model used to develop gridded meteorological fields and ii) CALPUFF- a non-steady-state Lagrangian puff model. Development of model inputs is discussed in two parts; CALMET modeling options and input development and CALPUFF modeling options and input development.

5.3.1 Modeling Option and Development of Model Inputs

(1) CALMET

CALMET is a diagnostic meteorological model which includes a wind field module which contains an objective analysis scheme and parameterized treatments of slope flows, kinematic terrain effects, terrain blocking effects, and a divergence minimization procedure, and a micrometeorological model for overland and overwater boundary layers. The model will produce for this application three-dimensional gridded fields of u, v, and w wind components, two-dimensional fields of Pasquill-Gifford-Turner stability class, surface friction velocity, mixing height, Monin-Obukhov length, and convective velocity scale and values of temperature, air density, short-wave solar radiation, and relative humidity defined at the surface meteorological stations. These fields are then used as input to the CALPUFF model.

The development of model inputs such as ones listed below are shown in Data book, pp. D5-5 to D5-8.

- Upper-Air Data
- Surface Data
- Geophysical Data
- Number of Vertical Layers
- Wind Field Options
- Other Modeling Options

(2) CALPUFF

CALPUFF is a multi-layer, multi-species non-steady-state Lagrangian puff dispersion model that can simulate the effects of time-and space-varying meteorological conditions on pollutant transport, transformation, and removal. In this application CALPUFF uses the three dimensional meteorological fields developed by the CALMET model. An another key feature used in this application is the module for treatment of complex terrain effects. The model produces hourly averaged concentrations ($\mu g/m^3$) at both gridded and discrete receptors. Results presented are for 24-hour averages.

1) Emission Inputs

All sources were modeled as point, area or volume sources. Heating season operating emission rates were used for major and medium size stationary sources as reported in the survey response answers from the Questionnaire on Stationary Source Emission Inventory as distributed by the MOE. These facilities were modeled as point sources. Emissions were prepared in spreadsheet format for SO_2 in a format for direct input to the ISC3 model. Input locations for the major and medium size point sources are specified in local Gauss-Krieger coordinate system, along with the emission rate in g/s, and stack parameters stack height, stack temperature, stack exit velocity, stack diameter. Emissions were adjusted for operating schedules as specified in the inventory. These ranged from 24-hour operations to 8-hour operating periods.
Table 5.11 identifies the heating season operating emission rates by source category.

Table 5.11 Operating SO_2 Emission Rates for Major and Medium Size Stationary Point Sources Used in the CALPUFF Modeling

Source Category	Operating Emission Rate (g/s)
Heating Plants	370
Combustion Sources	439
Area Sources	150
Total	959

2) Modeling Options

- Vertical distribution in the near-field is Gaussian
- ISC-type terrain adjustment
- No sub-grid-scale terrain adjustment

- No sub-grid-scale terrain adjustment
- Near-field puffs modeled as elongated slugs
- Transitional plume-rise modeled, stack-tip downwash included
- Puff-splitting allowed
- No chemical transformation of SO_2 to the sulfate aerosol was performed
- Vertical wind shear modeled above stack top
- No wet or dry deposition
- Used urban dispersion curves for grid-cell locations in urban locations, elsewhere rural dispersion curves were applied
- Buoyancy-induced dispersion included
- Partial plume penetration
- Minimum wind speed (m/s) for non-calm conditions was set at 0.5 m/s
- If puffs stay within the modeling domain after being split initially, they are allowed to split again around sunset before nocturnal shear develops. The time for this resplitting is at 1,600 during this winter episode.

3) Modeling Grid

The same vertical and horizontal grid used in CALMET (meteorological grid) will also be applied in the CALPUFF (computational grid) application. In addition, the sampling (receptor) grid will be at 1 km resolution which is identical to the computational grid.

4) Receptor Placement

Receptors were placed in a uniform Cartesian gridded array covering the entire modeling domain at 1,000 m horizontal resolution. Discrete receptors were placed at the nine RHI and seven IPH existing measurement points. The local Gauss-Krieger coordinates were determined from location maps provided by the Macedonian side.

5.3.2 Output Results and Model Verification

(1) Air Quality Data for Model Verification

1) Modeling Result of Present Air Quality

In the Study reported operating emissions were used to model SO_2 concentrations within Skopje. Because the emissions modeled are based on operating rates more likely characteristic of near peak emission rates, it is likely the model will overpredict

the observed concentrations. Day-specific hourly emission rates based on fuel consumption or power produce for the 15-20 highest SO_2 emission sources would likely significantly improve model performance. Modeling results are compared with monitored 24-hour SO_2 concentrations in Table 5.12 for both January 14 and 15, 1998.

2) Source Contribution

Figures 5.12 and 5.13 show the spatial distribution of the 24-hour SO_2 modeled concentrations for January 14 and 15, 1998. Table 5.13 shows the source contribution by source type for the discrete receptors (16 measurement points) on January 14 and 15, 1998. These results show that for the two points with the highest SO_2 concentration (HMI-Karpos and Hotel Panorama) that the major source contribution was from combustion sources other than the heating plants. Areawide emissions of SO_2 appear to contribute from 20 to 60% of the modeled concentration. Hourly-specific emissions, from sources other than the heating facility, would likely lower overall concentrations significantly. The areawide patterns are shown in Figures 5.12 and 5.13.

Table 5.12 Comparisons of Base Year 24-hour Average SO_2 Concentrations (in $\mu g/m^3$): CALPUFF Predictions vs. Observed Values

Jan. 14, 1998

Receptor Name	UTM X	UTM Y	Predicted	Observed
RHI Points				
AMSM	535.18	4650.15	512.7	91.0
Fruit Farming Institute - K. Voda	537.45	4648.25	346.1	NA
HMI - Karpos	533.65	4652.60	220.7	81.0
Dracevo - K. Voda	541.50	4647.00	204.7	NA
Avtokomanda - G. Baba	538.80	4651.00	413.6	133.0
Karpos IV - Karpos	532.80	4651.25	628.8	42.0
University Lib - Center	536.85	4650.55	215.1	73.0
J. B. Tito	535.90	4650.20	249.1	NA
Novo Lisice	539.60	4648.85	263.6	62.0
IPH Points				
Pivara	538.40	4650.10	261.0	94.5
Jane Sandanski (Kinder Galten)	538.70	4649.25	215.3	120.4
Cement Factory	538.30	4647.40	485.7	117.6
Hotel Panorama (Recreation Zone)	535.40	4648.95	337.2	110.3
Elementary School Dimo Hadzi Dimov	531.50	4651.35	174.8	111.9
DDD Station	537.50	4652.75	201.6	90.3
Municipal Health Institute	536.85	4649.30	255.5	106.9

Jan. 15, 1998

Receptor Name	UTM X	UTM Y	Predicted	Observed
RHI Points				
AMSM	535.18	4650.15	485.7	124.0
Fruit Farming Institute - K. Voda	537.45	4648.25	405.1	NA
HMI - Karpos	533.65	4652.60	374.4	120.0
Dracevo - K. Voda	541.50	4647.00	379.0	NA
Avtokomanda - G. Baba	538.80	4651.00	516.7	130.0
Karpos IV - Karpos	532.80	4651.25	792.0	76.0
University Lib - Center	536.85	4650.55	430.9	114.0
J. B. Tito	535.90	4650.20	515.4	NA
Novo Lisice	539.60	4648.85	507.6	59.0
IPH Points				
Pivara	538.40	4650.10	469.6	124.3
Jane Sandanski (Kinder Galten)	538.70	4649.25	600.5	121.7
Cement Factory	538.30	4647.40	419.3	107.0
Hotel Panorama (Recreation Zone)	535.40	4648.95	958.0	188.1
Elementary School Dimo Hadzi Dimov	531.50	4651.35	533.6	102.9
DDD Station	537.50	4652.75	337.5	90.8
Municipal Health Institute	536.85	4649.30	523.9	120.3

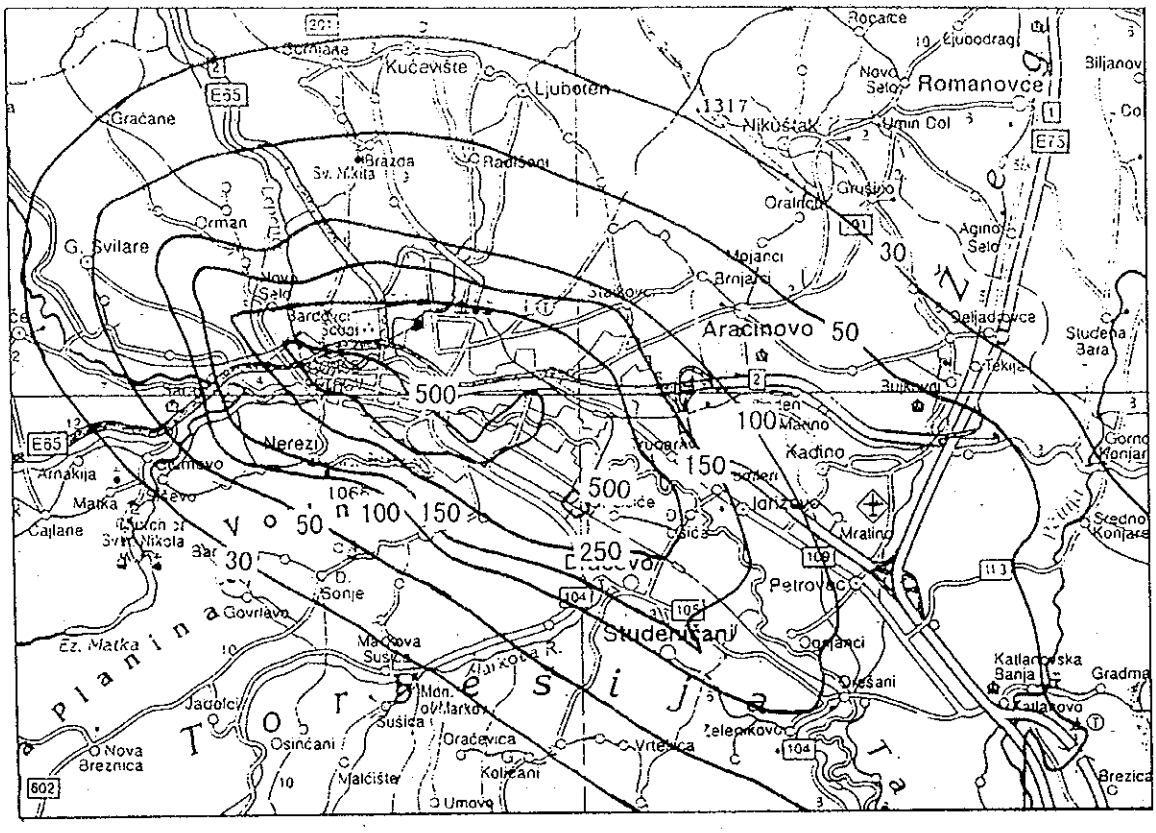

Figure 5.12 24-hour Average Spatial Distribution of SO_2 for January 14, 1998

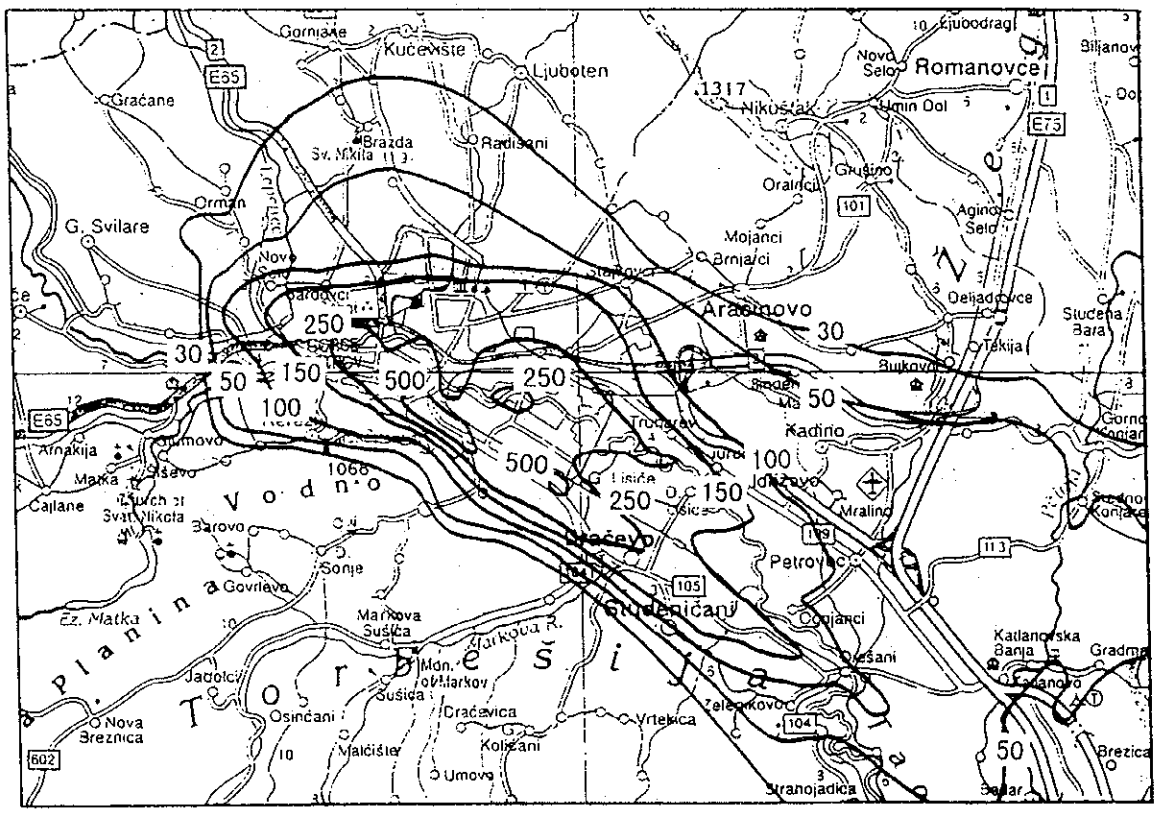

Figure 5.13 24-hour Average Spatial Distribution of SO_2 for January 15, 1998

Table 5.13 (1) Source Contributions of 1998 24-hour SO_2 Average Concentrations (in $\mu g/m^3$): at Discrete Receptor Locations

Jan. 14, 1998

Receptor Name	UTM X	UTM Y	Concentrations				Percent of Total Concentrations			
			Heating Plants	Combustion Sources	Volume Sources	Area Sources	Heating Plants	Combustion Sources	Volume Sources	School Heating Sources
RHI Points										
AMSM	535.18	4650.15	8.76	384.67	117.97	1.29	1.7%	75.0%	23.0%	0.3%
Fruit Farming Institute - K. Voda	537.45	4648.25	44.58	157.72	140.05	3.78	12.9%	45.6%	40.5%	1.1%
HMI - Karpos	533.65	4652.60	60.25	27.84	131.49	1.13	27.3%	12.6%	59.6%	0.5%
Dracevo - K. Voda	541.50	4647.00	18.14	53.27	128.91	4.43	8.9%	26.0%	63.0%	2.2%
Avtokomanda - G. Baba	538.80	4651.00	28.33	247.01	124.65	13.65	6.8%	59.7%	30.1%	3.3%
Karpos IV - Karpos	532.80	4651.25	463.46	49.63	114.65	1.03	73.7%	7.9%	18.2%	0.2%
University Lib - Center	536.85	4650.55	42.89	25.55	143.05	3.59	19.9%	11.9%	66.5%	1.7%
J. B. Tito	535.90	4650.20	12.64	106.25	127.13	3.07	5.1%	42.7%	51.0%	1.2%
Novo Lisice	539.60	4648.85	39.46	76.49	141.86	5.75	15.0%	29.0%	53.8%	2.2%
IPH Points										
Pivara	538.40	4650.10	28.94	96.45	132.15	3.41	11.1%	37.0%	50.6%	1.3%
Jane Sandanski (Kinder Galten)	538.70	4649.25	28.61	34.62	148.37	3.72	13.3%	16.1%	68.9%	1.7%
Cement Factory	538.30	4647.40	7.76	346.81	129.16	1.93	1.6%	71.4%	26.6%	0.4%
Hotel Panorama (Recreation Zone)	535.40	4648.95	6.12	213.57	116.51	0.95	1.8%	63.3%	34.6%	0.3%
Elementary School Dimo Hadzi Dimov	531.50	4651.35	39.39	16.83	116.26	2.30	22.5%	9.6%	66.5%	1.3%
DDD Station	537.50	4652.75	19.96	45.90	118.10	17.61	9.9%	22.8%	58.6%	8.7%
Municipal Health Institute	536.85	4649.30	33.91	76.46	139.64	5.53	13.3%	29.9%	54.6%	2.2%

Table 5.13 (2) Source Contributions of 1998 24-hour SO_2 Average Concentrations (in $\mu g/m^3$): at Discrete Receptor Locations

Jan. 15, 1998

Receptor Name	UTM X	UTM Y	Concentrations				Percent of Total Concentrations			
			Heating Plants	Combustion Sources	Volume Sources	Area Sources	Heating Plants	Combustion Sources	Volume Sources	School Heating Sources
RHI Points										
AMSM	535.18	4650.15	59.30	245.80	176.06	4.57	12.2%	50.6%	36.2%	0.9%
Fruit Farming Institute - K. Voda	537.45	4648.25	59.99	158.77	180.63	5.70	14.8%	39.2%	44.6%	1.4%
HMI - Karpos	533.65	4652.60	111.23	80.86	177.27	5.03	29.7%	21.6%	47.3%	1.3%
Dracevo - K. Voda	541.50	4647.00	62.26	145.68	166.53	4.57	16.4%	38.4%	43.9%	1.2%
Avtokomanda - G. Baba	538.80	4651.00	48.01	272.01	169.87	26.77	9.3%	52.6%	32.9%	5.2%
Karpos IV - Karpos	532.80	4651.25	395.67	226.84	166.33	3.16	50.0%	28.6%	21.0%	0.4%
University Lib - Center	536.85	4650.55	93.25	140.38	190.78	6.45	21.6%	32.6%	44.3%	1.5%
J. B. Tito	535.90	4650.20	67.35	262.26	179.52	6.27	13.1%	50.9%	34.8%	1.2%
Novo Lisice	539.60	4648.85	197.73	113.86	189.25	6.81	39.0%	22.4%	37.3%	1.3%
IPH Points										
Pivara	538.40	4650.10	112.96	169.33	180.61	6.74	24.1%	36.1%	38.5%	1.4%
Jane Sandanski (Kinder Galten)	538.70	4649.25	285.36	119.50	189.58	6.07	47.5%	19.9%	31.6%	1.0%
Cement Factory	538.30	4647.40	38.18	202.38	175.31	3.40	9.1%	48.3%	41.8%	0.8%
Hotel Panorama (Recreation Zone)	535.40	4648.95	44.82	738.94	170.49	3.77	4.7%	77.1%	17.8%	0.4%
Elementary School Dimo Hadzi Dimov	531.50	4651.35	261.31	101.52	167.39	3.37	49.0%	19.0%	31.4%	0.6%
DDD Station	537.50	4652.75	42.70	100.81	173.58	20.45	12.6%	29.9%	51.4%	6.1%
Municipal Health Institute	536.85	4649.30	89.28	241.76	185.60	7.24	17.0%	46.1%	35.4%	1.4%

(2) Future Year and Emission Control Scenario Modeling Results - CALPUFF

1) Future Scenario

Model inputs for the future year simulation are identical to base year modeling effort with the exception of changes to the emission inputs. For the future year (2008) each stationary point source was increased by 20% to reflect additional industrial growth, while area sources remained constant. The control scenario was to switch from oil to natural gas for all of Skopje heating plants. Emissions from the heating facilities were reduced by 80% under this control scenario.

2) Modeling Results and Source Contribution

Figures 5.14 and 5.15 show the 24-hour average spatial distribution of SO_2 for January 14 and 15 with implementation of the control strategy. Table 5.14 shows the source contribution by source type for the discrete receptors (16 measurement points) for both days of the future-year with the control strategy implemented. Because the peak modeled SO_2 measurement points (Hotel Panorama) had almost no contribution from the heating plants the control strategy shows a net increase from the base year because of the growth in emissions from combustion sources. On the other hand, the measurement point that saw the biggest net reduction in average concentration of 313 $\mu g/m^3$ was Karpos IV because almost three-quarters of the concentration in the base year is attributable to emissions from the heating plants.

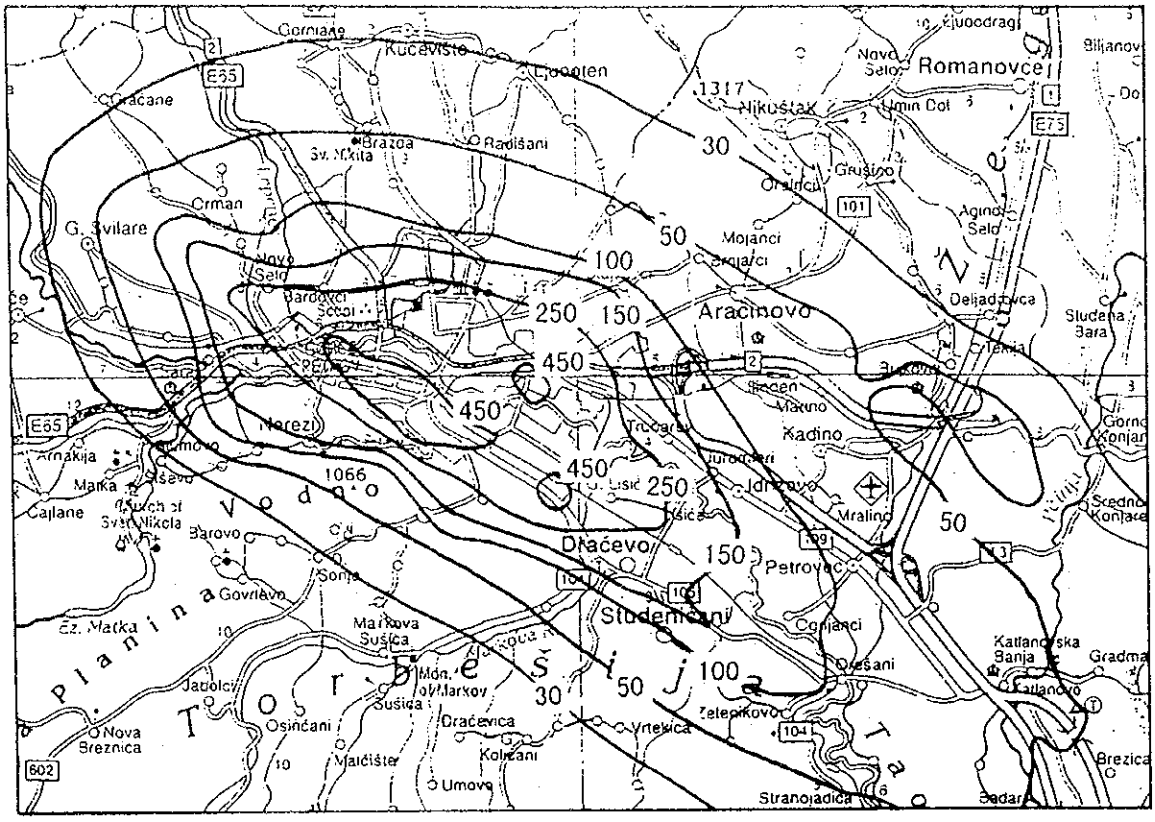

Figure 5.14 24-hour Average Spatial Distribution of SO_2 for January 14, 2008

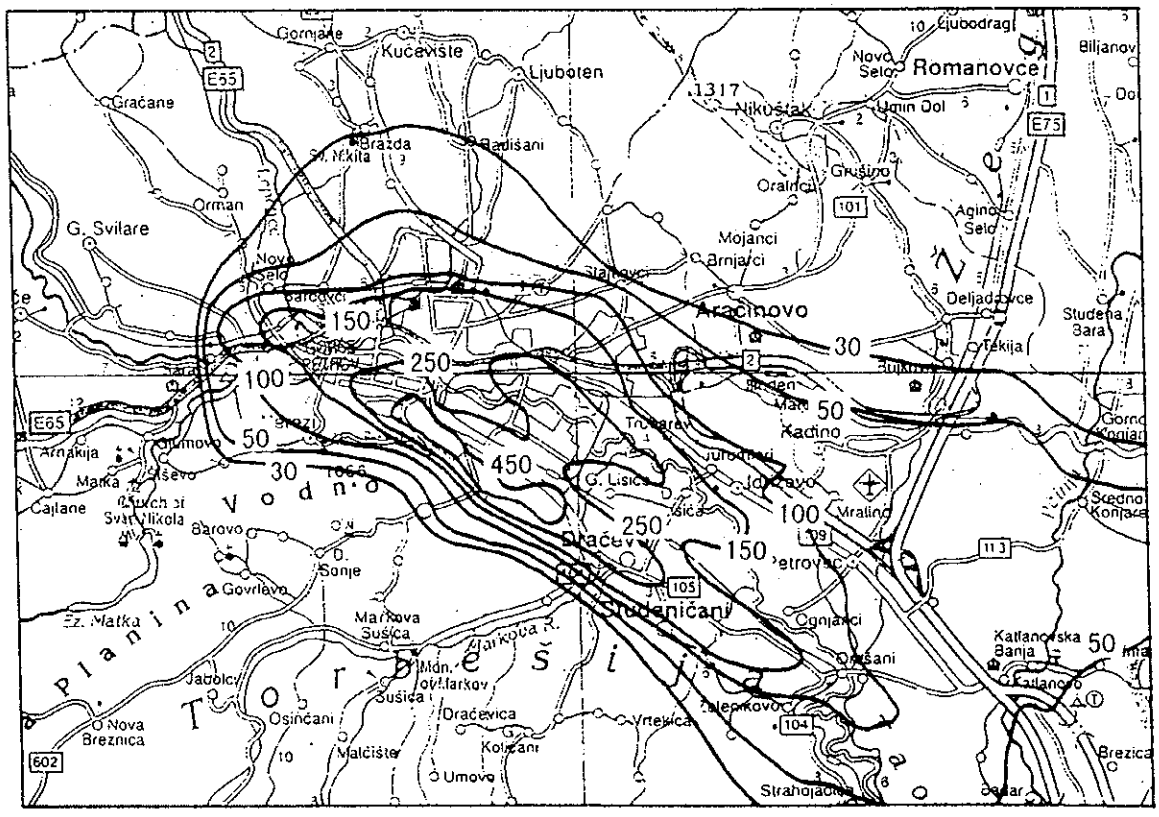

Figure 5.15 24-hour Average Spatial Distribution of SO_2 for January 15, 2008

Table 5.14 (1) Source Contributions of 2008 24-hour SO_2 Average Concentrations (in $\mu g/m^3$): at Discrete Receptor Locations

Jan. 14,

Receptor Name	UTM X	UTM Y	Concentrations				Percent of Total Concentrations			
			Heating Plants	Combustion Sources	Volume Sources	Area Sources	Heating Plants	Combustion Sources	Volume Sources	School Heating Sources
RHI Points										
AMSM	535.18	4650.15	1.75	461.60	117.97	1.29	0.3%	79.2%	20.2%	0.2%
Fruit Farming Institute - K. Voda	537.45	4648.25	8.92	189.27	140.05	3.78	2.6%	55.3%	40.9%	1.1%
HMI - Karpos	533.65	4652.60	12.05	33.41	131.49	1.13	6.8%	18.8%	73.8%	0.6%
Dracevo - K. Voda	541.50	4647.00	3.63	63.93	128.91	4.43	1.8%	31.8%	64.2%	2.2%
Avtokomanda - G. Baba	538.80	4651.00	5.67	296.42	124.65	13.65	1.3%	67.3%	28.3%	3.1%
Karpos IV - Karpos	532.80	4651.25	92.69	59.56	114.65	1.03	34.6%	22.2%	42.8%	0.4%
University Lib - Center	536.85	4650.55	8.58	30.66	143.05	3.59	4.6%	16.5%	77.0%	1.9%
J. B. Tito	535.90	4650.20	2.53	127.50	127.13	3.07	1.0%	49.0%	48.9%	1.2%
Novo Lisice	539.60	4648.85	7.89	91.79	141.86	5.75	3.2%	37.1%	57.4%	2.3%
IPH Points										
Pivara	538.40	4650.10	5.79	115.74	132.15	3.41	2.3%	45.0%	51.4%	1.3%
Jane Sandanski (Kinder Galten)	538.70	4649.25	5.72	41.54	148.37	3.72	2.9%	20.8%	74.4%	1.9%
Cement Factory	538.30	4647.40	1.55	416.18	129.16	1.93	0.3%	75.8%	23.5%	0.4%
Hotel Panorama (Recreation Zone)	535.40	4648.95	1.22	256.29	116.51	0.95	0.3%	68.3%	31.1%	0.3%
Elementary School Dimo Hadzi Dimov	531.50	4651.35	7.88	20.19	116.26	2.30	5.4%	13.8%	79.3%	1.6%
DDD Station	537.50	4652.75	3.99	55.08	118.10	17.61	2.0%	28.3%	60.6%	9.0%
Municipal Health Institute	536.85	4649.30	6.78	91.75	139.64	5.53	2.8%	37.6%	57.3%	2.3%

Table 5.14 (2) Source Contributions of 2008 24-hour SO_2 Average Concentrations (in $\mu g/m^3$): at Discrete Receptor Locations

Jan. 15

Receptor Name	UTM X	UTM Y	Concentrations				Percent of Total Concentrations			
			Heating Plants	Combustion Sources	Volume Sources	Area Sources	Heating Plants	Combustion Sources	Volume Sources	School Heating Sources
RHI Points										
AMSM	535.18	4650.15	11.86	294.96	176.06	4.57	2.4%	60.5%	36.1%	0.9%
Fruit Farming Institute - K. Voda	537.45	4648.25	12.00	190.53	180.63	5.70	3.1%	49.0%	46.5%	1.5%
HMI - Karpos	533.65	4652.60	22.25	97.03	177.27	5.03	7.4%	32.2%	58.8%	1.7%
Dracevo - K. Voda	541.50	4647.00	12.45	174.82	166.53	4.57	3.5%	48.8%	46.5%	1.3%
Avtokomanda - G. Baba	538.80	4651.00	9.60	326.41	169.87	26.77	1.8%	61.3%	31.9%	5.0%
Karpos IV - Karpos	532.80	4651.25	79.13	272.21	166.33	3.16	15.2%	52.3%	31.9%	0.6%
University Lib - Center	536.85	4650.55	18.65	168.46	190.78	6.45	4.9%	43.8%	49.6%	1.7%
J. B. Tito	535.90	4650.20	13.47	314.71	179.52	6.27	2.6%	61.2%	34.9%	1.2%
Novo Lisice	539.60	4648.85	39.55	136.63	189.25	6.81	10.6%	36.7%	50.8%	1.8%
IPH Points										
Pivara	538.40	4650.10	22.59	203.20	180.61	6.74	5.5%	49.2%	43.7%	1.6%
Jane Sandanski (Kinder Galten)	538.70	4649.25	57.07	143.40	189.58	6.07	14.4%	36.2%	47.9%	1.5%
Cement Factory	538.30	4647.40	7.64	242.86	175.31	3.40	1.8%	56.6%	40.8%	0.8%
Hotel Panorama (Recreation Zone)	535.40	4648.95	8.96	886.73	170.49	3.77	0.8%	82.9%	15.9%	0.4%
Elementary School Dimo Hadzi Dimov	531.50	4651.35	52.26	121.82	167.39	3.37	15.2%	35.3%	48.5%	1.0%
DDD Station	537.50	4652.75	8.54	120.97	173.58	20.45	2.6%	37.4%	53.6%	6.3%
Municipal Health Institute	536.85	4649.30	17.86	290.11	185.60	7.24	3.6%	57.9%	37.1%	1.4%

5.4 Receptor Modeling of Suspended Particulate Matter

5.4.1 Aerosol Characterization Measurements

(1) Sampling of Aerosol

During the period from December 1997 through February 1998, supplemental measurements of fine particle concentrations were conducted in Skopje using the Anderson multistage impactor.
Samples were collected at the Republic Hydrometeorology Institute (RHI), underneath the RailWay Station (RWS) overpass, and in a residential area (Majcin Dom). The primary purpose of this sampling program was to provide aerosol characterization data for the assessment of source contributions to fine particulate matter concentrations.

(2) Analysis of Aerosol

Filters were analyzed gravimetrically for total mass accumulated, and were also subjected to elemental analysis by X-ray fluorescence (XRF). The results of this measurement exercise were mixed. Subjectively good agreement was observed between the time periods for which high mass concentrations were observed and concurrent SO_2 and black smoke measurements by the RHI. However, some compromised the value of the Anderson data. Many elements' observed concentrations are at or below the level of uncertainty in measurements, and it also cannot be assumed that ratios of elemental concentrations on a filter are accurate. Thus the elemental concentrations must be considered to be dimensionless values for purposes of analysis, and cannot be used in direct source apportionment calculations using existing source profiles and receptor modeling techniques.
Despite the limitations on interpretation of the elemental and mass measurements, it was possible to identify several consistent patterns in elemental ratios (and presumably, source contributions) using both graphical and statistical analyses.

5.4.2 Principal Component Analysis (PCA)

(1) Theory of PCA

PCA has been applied in many studies with a fair-to-good degree of success to reveal sources, especially of urban aerosols. PCA is a statistical technique for examining the variance in a multivariate data set by identifying characteristic, recurring and independent modes of variation in a large data set. It is based on the assumption that

the variables can be represented as linear combinations of a set of mutually independent factors. The objective in PCA is to find a minimum number of factors that explain most of the variance of the system. In theory, the variance explained by each factor remains large for the several factors associated with important sources and drops sharply beyond. Interpretation of the factors is accomplished by examining the weight, called factor loading, of each variable in the linear combination that defines the factor. The square of the factor loading gives the fraction of a variable's total variance, which is accounted for by that factor. The sum of squares of the factor loadings of a variable is the communality (h^2), and it is the amount of a variable's total variance that may be attributed to the extracted factors. Often for the purpose of aiding the identification of the nature of the factors in a system, the matrix of factors is generally rotated. Varimax orthogonal rotation is commonly applied.

(2) The Source of Targets for PCA

To estimate the sources of the trace elements measured at the three points (RHI, M. Dom and RWS) the Study Team performed PCA with the help of the Easy Factor Analysis (EFA Version 2.5) program package (Fuerst, 1988). Some of the problems encountered in the Study were lack of source profiles specific to the area and the limited sample size. The atmosphere in a less-industrialized city and in rural areas is expected to be less complex relative to urban atmospheres of most industrialized nations. Hence PCA can be applied, at least qualitatively, to determine sources of pollution impacting the points under study even in the absence of source profiles specific to the area. Because PCA works through the identification of variability of multiple factors in a dataset, the measurements were conducted at the three points (RHI, M. Dom, and RWS) to attempt to collect samples that were higher or lower in contributions from different known source types. Anticipated source types included mobile sources (the RWS data were specifically collected under the underpass to achieve maximum impact from exhaust and road dust), heating sources (district heating plants and residential and combustion of oil, as well as woodburning), and industrial sources (cement plants and metallurgy).

(3) Chosen Elements for PCA

Fifteen elements (Na, Mg, Al, Si, S, Cl, K, Ca, Ti, V, Mn, Fe, Zn, Br, Pb) were initially chosen for analysis with PCA. Uncertainties of the other elements reported by XRF were consistently larger than their reported values, and could not be used. With this set of 15 elements, PCA was unable to resolve or separate the sources. This was suspected to be due to the large measurement uncertainties associated with some of these elements (Na, Mg and Ti) leading to unstable results. This could also be due

to multi-collinearity arising from the presence of two or more emission sources with very similar source signatures. PCA was performed again on using the data for the remaining twelve elements. A total of 56 samples collected between December 25, 1997 to February 21, 1998 were used for the analysis. The results are summarized below.

Table 5.15 provides the measurement range, means and standard deviation of the elemental concentrations (in $\mu g/m^3$). Ca has a high standard deviation due to the anomalous large concentration observed on February 17. The concentrations of other elements were higher as well on this day. The high fluctuation in Br average in the present data is not surprising as Br concentrations can be considerably influenced by local Br emissions from automobile exhaust.

Table 5.15 Mean Elemental Measured Concentration* and Standard Deviation

($\mu g/m^3$)

	Mean	Std. Deviation		Mean	Std. Deviation
Al	102.81	118.52	V	0.27	0.19
Si	729.63	1512.23	Mn	0.46	0.52
S	72.27	120.01	Fe	3.46	4.87
Cl	12.16	39.99	Zn	0.32	0.36
K	23.16	45.59	Br	0.54	1.24
Ca	60.79	194.69	Pb	2.28	4.00

* See text for discussion of measurement bias. The values reported are nominally nanograms per cubic meter ($10^{-9}g/m^3$) but each element's concentrations are subject to an undetermined negative bias in measurement.

(4) Correction Coefficient of the Elements

The matrix for linear correlation coefficients for the 56 samples is given in Table 5.16. For 'n' =56, correlation coefficient (r) greater than 0.35 in this matrix indicate a statistically significant (p=0.01) relationship. However, only a 'r' value greater than 0.7 would indicate that at least 50% of the variability can be explained by a linear association between the two variables. Good correlation is observed between S, Cl, K, Ca and Fe, suggesting that these elements were carried together in the same air mass, either because they arise from a single type of source, or because the spatial and temporal distributions of emissions from contributing source types are similar in Skopje. Particulate sulfur is expected to be primarily the result of secondary sulfate, whose origin is SO_2 from the combustion of fuel oil. Potassium (K) is known to be more abundant in smoke from woodburning. These two findings suggest that the

correlation of S and K arise from stagnation conditions in cold weather, resulting in an accumulation in the atmosphere over Skopje of concentrations of heating source emissions over a long enough time period for some fraction of the SO_2 to oxidize to sulfate (one to two days). Ca and Fe are not commonly associated with heating sources, and thus may represent another source of fine particles that accumulate during stagnation (cement manufacturing is a possibility here).

Table 5.16 Correlation Matrix Describing the Correlations Between the Measured Variables

	Al	Si	S	Cl	K	Ca	V	Mn	Fe	Zn	Br	Pb
Al	1.00	0.78	0.73	0.48	0.73	0.47	0.79	0.66	0.66	0.55	0.35	0.38
Si	0.78	1.00	0.74	0.47	0.80	0.47	0.58	0.61	0.58	0.55	0.18	0.22
S	0.73	0.74	1.00	0.89	0.98	0.89	0.75	0.62	0.86	0.63	0.59	0.59
Cl	0.48	0.47	0.89	1.00	0.90	0.99	0.55	0.34	0.85	0.54	0.72	0.70
K	0.73	0.80	0.98	0.90	1.00	0.90	0.69	0.56	0.86	0.63	0.57	0.58
Ca	0.47	0.47	0.89	0.99	0.90	1.00	0.55	0.36	0.84	0.52	0.69	0.68
V	0.79	0.58	0.75	0.55	0.69	0.55	1.00	0.61	0.74	0.51	0.53	0.54
Mn	0.66	0.61	0.62	0.34	0.56	0.36	0.61	1.00	0.60	0.49	0.38	0.38
Fe	0.66	0.58	0.86	0.85	0.86	0.84	0.74	0.60	1.00	0.71	0.87	0.87
Zn	0.55	0.55	0.63	0.54	0.63	0.52	0.51	0.49	0.71	1.00	0.57	0.70
Br	0.35	0.18	0.59	0.72	0.57	0.69	0.53	0.38	0.87	0.57	1.00	0.98
Pb	0.38	0.22	0.59	0.70	0.58	0.68	0.54	0.38	0.87	0.70	0.98	1.00

There is also a good correlation between Al, Si, K, V, Mn and Fe. Fe, Mn and K are all present in the aluminosilicate phase (e.g., crustal dust or rock). Also, as expected, Br and Pb show a strong correlation, as both are present in fixed ratios in the exhaust of vehicles fueled with leaded gasoline.

(5) Communality of Elements

Factor extraction using principal components, orthogonal varimax rotation, retention of factors with eigenvalues > 1.00, communality estimation from factors after one iteration and factor scores are the defaults of the EFA program. In these analyses of the number of factors, 'm' is decided by the eigenvalue cutoff. As the cutoff value decreases, 'm' increases. On the selection of the cutoff value, Hopke et al., (1985) pointed out that there is no universally applicable method for establishing 'm' and it is necessary to discard a number of small eigenvalues. In order to establish probable number of source factors, we used different eigenvalue cutoffs. With an eigenvalue

cutoff of 0.5 a four-factor solution was obtained which accounted for 93.5% of the total variance of the measured parameters and was consistent with the correlation matrix. Communality was close to unity for most elements.

(6) Four-factor Solution

Results from the four-factor solution are discussed.

1) Factor 1

Factor 1, which accounts for 25% of the variance of this four-factor solution, has a high loading of Pb, Br and is clearly representing the contributions of mobile sources. It also includes a moderate loading of Fe, but the origin of this is not certain. Some road dust (earth crustal) elements would be expected to be present with vehicle exhaust, but it is also possible that there is a source whose emissions are abundant in Fe near the railway station where the highest Pb and Br concentrations were observed.

2) Factor 2

Factor 2 has strong loadings from Al, Si, K, V, and Mn and explains 29% of the total variability. This probably represents the crustal component as Al, Si, K, and Mn are all present in the aluminosilicate phase (e.g., crustal dust or rock) and hence can be termed as the 'soil' factor. The sources of this material could be windblown dust, construction dust, or regional background concentrations. The occurrence of V in this grouping is somewhat unusual as V has more commonly been used as an indicator species for fuel oil combustion. Direct collection of source profiles for crustal material in different areas of Skopje would be instructive in determining if there is a separate source of V.

3) Factor 3

Factor 3, with high loadings of S, Cl, K, and Ca is more complex and is harder to interpret. It represents the largest portion of the aerosols (30% of the variance explained by this factor). As previously noted, particulate S is expected to be dominated by secondary sulfate during stagnation events. As aerosol concentrations during such events are likely to be a well-mixed combination of all sources of particulate matter (especially "fine mode" particles smaller than 2.5 microns), this factor is likely to include both combustion sources (S from fuel oil, K and possibly Cl from firewood) and other sources. Ca could be indicating contributions from either crustal material or cement manufacturing.

4) Factor 4

Factor 4 contained only Zn and accounted for about 10% of the variance. Both Zn and Sb have been reported to be relatively abundant in the emissions from municipal waste incineration. This factor could indicate contributions due to burning household refuse, or commercial facility waste incineration. Emissions from this source are not identified in the emission inventory, but should be investigated.
Table 5.17 gives the results of the four-factor solution.

Table 5.17 Principal Component Analysis of Elemental Concentrations in Skopje

	Rotated Factor Loadings				
	Factor 1	Factor 2	Factor 3	Factor 4	Communality
Al	0.10	0.85	0.30	0.21	86.08
Si	-0.16	0.70	0.44	0.46	92.17
S	0.27	0.55	0.75	0.19	97.11
Cl	0.43	0.18	0.87	0.11	99.07
K	0.22	0.50	0.79	0.26	99.73
Ca	0.41	0.19	0.88	0.08	98.27
V	0.38	0.79	0.30	-0.05	85.45
Mn	0.24	0.82	0.06	0.16	76.03
Fe	0.65	0.47	0.54	0.21	96.87
Zn	0.47	0.32	0.22	0.76	95.43
Br	0.91	0.16	0.34	0.07	97.01
Pb	0.91	0.16	0.30	0.22	98.81

In summary, the PCA results indicate that four source groupings can be observed as contributors to SPM concentrations in Skopje. The specific source categories that are apparent, based on knowledge of elemental abundances in emissions, include mobile sources, earth crustal material, heating with fuel oil and firewood, and potentially refuse incineration. The elements providing the most useful information in identifying the principal components included Pb, Br, Al, Si, K, V, Mn, S, and Zn.

5.4.3 Source Profile Development from PCA Results

(1) Analysis of Source Elemental Profile

A problem with the direct use of PCA results is that they are based on normalized variables and apportion variance. This means that the analysis does not directly provide results analogous to the source profiles used in chemical mass balance (CMB)

receptor modeling. Several investigators have used PCA to identify the key elements associated with a source and then perform a multiple regression analysis of the mass against those elemental concentrations. Thurston and Spengler (1982) have suggested another approach. They developed a method, Absolute Principal Component Scores (APCS), for extracting factor compositions; so that the results are in the same form as results from CMB. By regressing sample particle mass concentration on the APCS for each sample, they derived each source's estimated mass concentration. The pollution source elemental profiles implied by the estimated source impacts are then derived using linear regression. Subsequently applying the derived source elemental profiles to the source mass contributions at the measurement point allows an elemental mass balance to be estimated.

(2) Source Mass Contribution

Table 5.18 provides the mean mass contributions obtained from PCA identified sources. The results in Table 5.18 indicate that there is an unexplained mass of 148.1 mg/m^3, which is more than the sum of mass of all the sources accounted for by this regression. There are two factors that yield this result. First, the negative bias in XRF analyses results in nominal elemental concentrations that are perhaps a fraction of a percent of the actual values. Second, XRF does not provide mass estimates for lighter elements, including carbon, and elemental and organic carbon (EC and OC) are commonly found to represent half or more of total fine particle concentrations.
A small number of concurrent samples were collected and analyzed for elemental and organic carbon, but the small number of samples, and the previously described difficulties in measurement, preclude the use of the carbon data in this analysis. Thus, the magnitude of the unexplained mass is largely meaningless. In this analysis, an overall R^2 of 0.97 was obtained. The estimated impacts are dominated by the 'soil' and the 'heating' components (about 16 and 14 % respectively). Motor vehicles and incineration each average 2.5 and 6.9% of the total mass. Again, however, the mass values reported for individual species have a constant negative, but unknown bias due to the nonuniform deposits on filters.

Table 5.18 Mean Mass Contributions from PCA-identified Sources

Source	Mean Particle Source Contribution ($\mu g/m^3$ ± Standard Error of mean)
Motor Vehicles	6.2 (±1.4)
Soil	39.0 (±1.4)
Heating	34.5 (±1.4)
Refuse Incineration	17.1 (±1.4)
Unexplained	148.1 (±9.0)

Table 5.19 displays the percentage elemental compositions resulting from the regression of elemental concentrations on the source mass contributions. Elements missing from a profile were not found to have statistically significant regression coefficients when regressed on that source category's mass impacts. The relative abundance of specific elements suggests that these profiles do in fact represent mixtures of sources. For example, although the occurrence of crustal materials in the "motor vehicle" profile can be explained, the presence of K and Cl would not be expected. It is possible, however that as the highest Pb and Cl values were obtained in a small number of samples collected at the RWS sources of woodsmoke could cause an apparent association of these elements with mobile source emissions. Table 5.20 contains the elemental impacts distributed among the sources, as calculated from the mass contribution estimates from Table 5.18 and the elemental profiles in Table 5.19 comparison with the concentrations shown in Table 5.15, shows overprediction of elemental contributions but general agreement in magnitude for different elements.

Table 5.19 PCA-derived Trace Element Source Profiles (% of mass ± S.E.)

Element	Motor Vehicle	Soil	Heating	Incineration
Al	0.0020 ±0.0010	0.0026 ±0.0010	0.0010 ±0.0002	0.0015 ±0.0004
Si		0.0271 ±0.0015	0.0193 ±0.0017	0.0416 ±0.0035
S	0.0031 ±0.0005	0.0017 ±0.0001	0.0036 ±0.0001	0.0014 ±0.0002
Cl	0.0028 ±0.0001	0.0002 ±0.0001	0.0010 ±0.0001	0.0003 ±0.0001
K	0.0016 ±0.0001	0.0006 ±0.0001	0.0010 ±0.0001	0.0007 ±0.0001
Ca	0.0127 ±0.0006	0.0010 ±0.0001	0.0050 ±0.0001	0.0010 ±0.0002
V	0.00001			
Mn	0.00002	0.00001		
Fe	0.0005 ±0.0001	0.0001 ±0.0000	0.0001 ±0.0000	0.0001±0.0000
Zn	0.00003			0.00002
Br	0.0002 ±0.0000			
Pb	0.0006 ±0.0000			0.0001 ±0.0000

Table 5.20 Mean Source Contributions to Coarse Elemental Concentrations ($\mu g/m^3$)

	Motor Vehicles	Soil	Heating	Incineration
Al	12.46	101.296	34.53	25.65
Si		1055.816	666.429	701.1
S	19.313	66.232	89.778	23.94
Cl	17.444	7.792	34.53	5.13
K	9.968	23.376	34.53	11.97
Ca	79.121	38.96	172.65	17.1
V	0.0623			
Mn	0.1246	0.3896		
Fe	3.115	3.896	3.453	1.71
Zn	0.1869			0.342
Br	1.246			
Pb	3.738			1.71

(3) Graphical Analysis of Selected Elemental Concentrations

The PCA results are suggestive of relationships between concentrations of different elements. For emissions processes that occur in a consistent manner (e.g., combustion of gasoline in motor vehicles), consistent ratios of certain elements are expected to be observed (e.g., the ratio of Pb to Br is determined by the relative amounts of Pb and Br in the gasoline itself). Scatterplots of element pairs can serve to convey the consistency of specific ratios across ambient measurements. Where elements are emitted by multiple sources, variability in ambient ratios would be expected. Several plots are shown below that serve to partially explain and confirm the preceding discussion of PCA analyses. As before, the concentrations shown include the effects of the variable negative bias in XRF analysis, however this bias does not appear to affect the ability to examine consistency in element ratios.

Figure 5.16 shows a scatterplot of Pb and Br concentrations. With the exception of a single point, the Pb/Br ratio is effectively constant for all data points. This suggests that there are no sources of either element other than motor vehicle exhaust. It was anticipated that under some conditions, long-range transport of Pb from the smelter at Veles might be observed, but this does not appear to be a factor in this dataset.

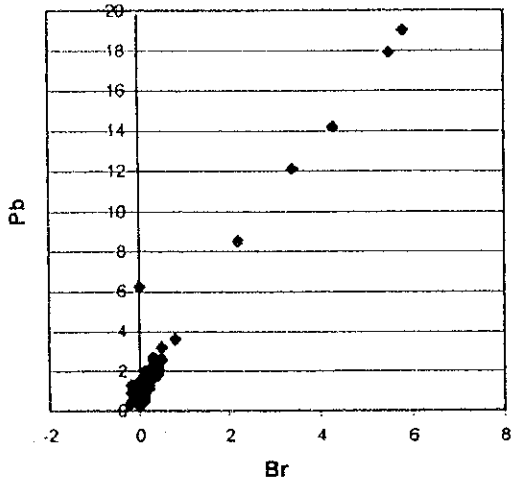

Figure 5.16 Pb vs. Br Scatterplot

Figure 5.17 shows the observed relationship between Pb and K. Here, there is substantially greater variability in ratios. The highest Pb concentrations, collected at the RWS, exhibit wide variability in Pb/K ratio. There appears to be a much greater consistency in ratios at lower concentrations (RHI and M. Dom) but these may be more a reflection of consistency in distribution of areawide emissions of sources of the two elements. Working on the assumption that the predominate source of K is woodburning, the fact that firewood and mobile source emissions are widely distributed would explain the general pattern observed.

Figures 5.18 and 5.19 show the relationship between crustal elements-Si, Fe, and Mn. Although clearly correlated, the broad range of ratios observed suggests either several different types of crustal materials or non-crustal sources of the metals.

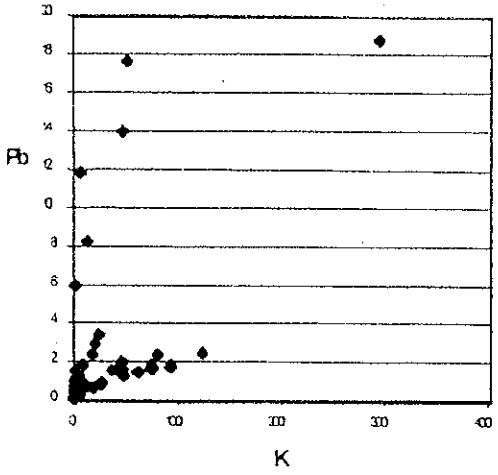

Figure 5.17 Pb vs. K Scatterplot

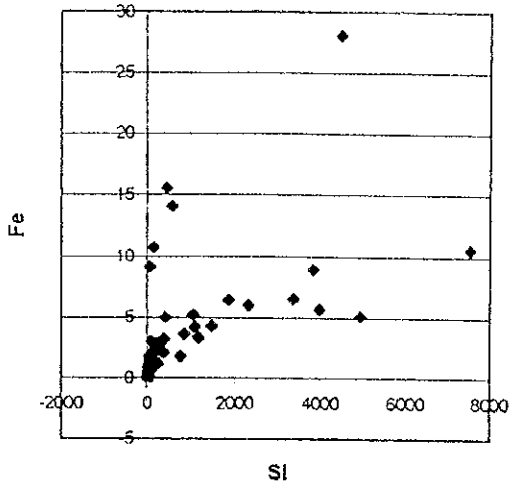

Figure 5.18 Fe vs. Si Scatterplot

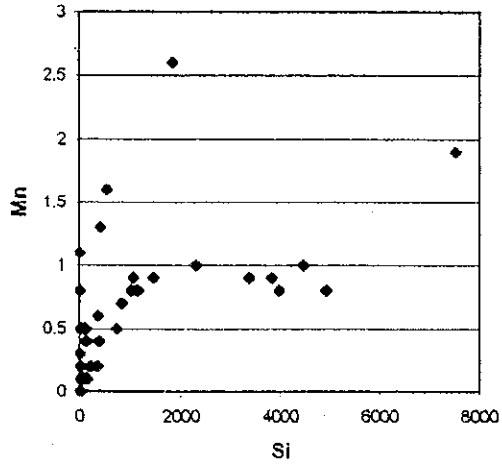

Figure 5.19 Mn vs. Si Scatterplot

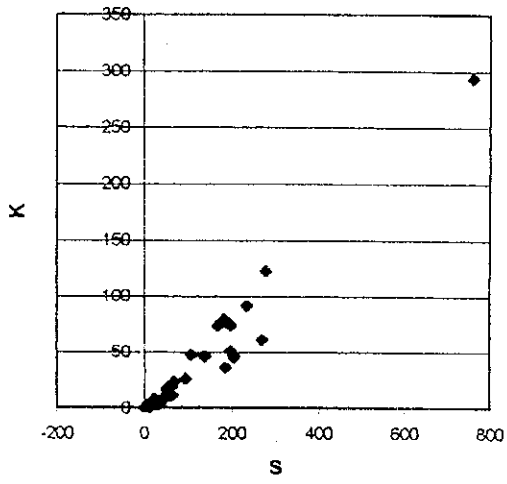

Figure 5.20 K vs. S Scatterplot

Figure 5.20 shows a strong relationship between K and S. As previously discussed, assuming that particulate sulfur is primarily in the form of secondary sulfate from heating, the strength of this relationship suggests that meteorological factors, specifically stagnation and cold temperatures, cause accumulation of heating emissions, with a relatively consistent ratio of firewood and fuel oil-burning source contributions.

Figure 5.21 shows the data obtained for V and S. The relationship is far less consistent than the K-S relationship, although the opposite would be expected if S and V are both primarily tied to fuel oil combustion. This provides further indication of a separate source of V influencing the observations.

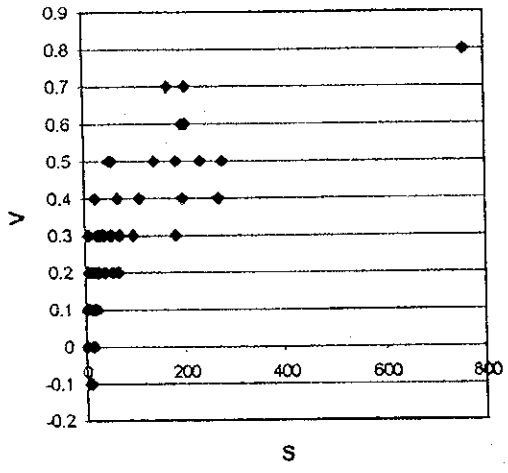

Figure 5.21 V vs. S Scatterplot

(4) Conclusions

There are clear indications of the importance of heating and mobile source contributions to SPM concentrations in Skopje. In particular, the data collected provide strong evidence of a significant secondary sulfate contribution during stagnation conditions. Elemental ratios and source profiles can be used to determine the actual concentration contributions of these sources, however additional sampling and chemical analyses are needed to provide a dataset that can be used to make this determination. The current dataset, because of the uncertainty in absolute elemental concentrations, can only be used to confirm the existence of anticipated relationships between species.

It is possible that both industrial and refuse incineration emissions are contributing to SPM concentrations in significant amounts, however it is not possible to identify these contributions without additional data. Source profiles for fuel oil combustion and road dust would be useful in allowing those portions of the SPM composition to be separately identified. If additional sampling and aerosol characterization studies are conducted, the results of the current analysis can be used to identify several of the key species that should be included. It would be desirable to include elemental and

organic carbon and direct determination of sulfate (as opposed to elemental sulfur), along with the other elements listed here, and others that have proven useful in other studies, but whose sensitivity in this dataset was to low to provide useful data. These species include As, Se, Cr, and Hg.

5.5 Air Pollution Control

5.5.1 Environmental Protection Measures

(1) Measures

1) Programs

Environmental protection measures can be divided into structural and non-structural programs.

The structural programs include installation of environmental conservation equipment and systems, conversion to low-polluting equipment and systems, energy saving measures and relocation of plants.

The non-structural programs include reduction in emission of pollutants by stricter enforcement of regulations, and enactment and stricter enforcement of related laws and ordinances. Examples are subsidy measures in the implementation of structural programs, and environmental education and training of the personnel of the concerned organizations. School education on environmental problems should be continuously done, starting from the elementary grades.

2) Structural Measures

For the stationary sources, the applicability of alternatives in control technology currently put into practice (as shown in Data Book, Table D2.2) will be reviewed. Those appropriate to the kind and scale of the sources will be studied in general terms.

For the automobile emission gas, the reduction method of SO_2, NOx, CO, HC, SPM and Pb is shown in Data Book, Table D2.3.

A large portion of the transport measures is common in Skopje and the Country, but consideration of the conversion from buses to the new traffic system is a goal at Skopje.

3) Non-structural Measures

As for factors contributing to the deterioration of environment, factors such as the

lack of environment protection equipment at plants and other facilities and incomplete measures can be singled out. Other factors are institutional problems and low awareness of the citizens on environmental problems and lack of fostering of personnel.

Personnel awareness is necessary in the combat against environment pollution. The first step to be taken in this direction is to reinforce awareness and enlightenment of ordinary citizens on environment protection, as well as to foster and retrain leaders so that they are able to perceive and evaluate environmental problems correctly. Figure 5.22 shows an example of public awareness program. To accomplish this, aggressive measures are needed, such as a training system for those concerned with environmental problems, seminars for various levels of people and school education starting from primary education. In the Country, however, fostering of personnel is still at its initial stage.

Personnel training are not practiced. Only since two years ago, the University of Skopje offered environmental engineering courses, which are lectured by professors in the field of industrial engineering, chemistry, machinery and biology.

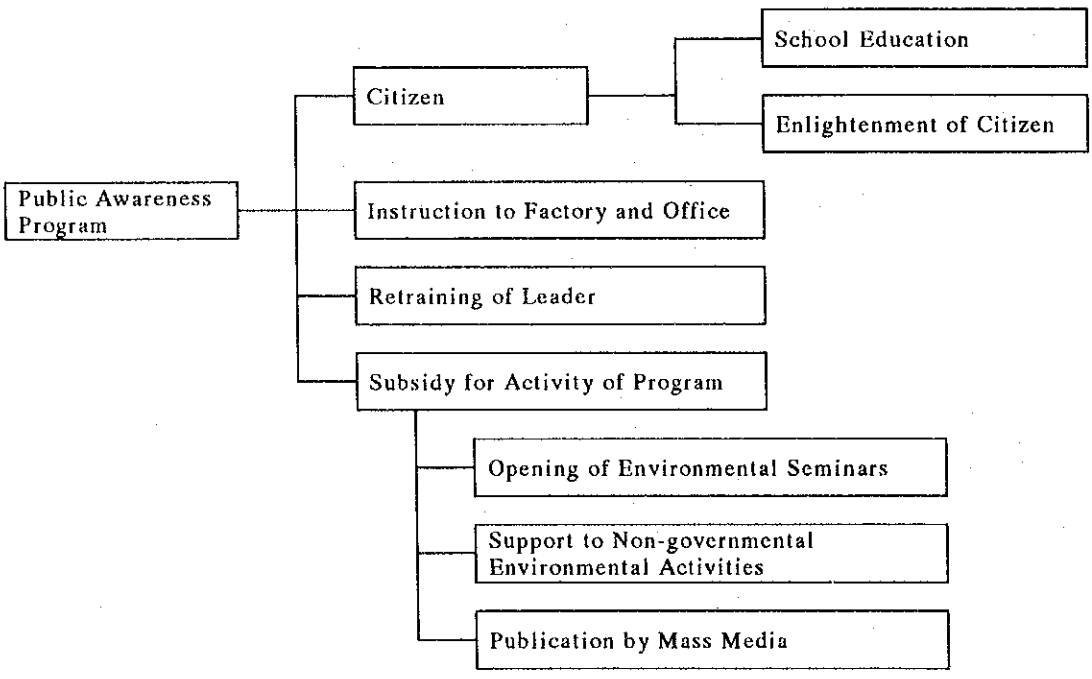

Figure 5.22 An Example of Public Awareness Program

(2) Introduction of Preventive Actions in Japan

The following preventive actions were effective against air pollution under local Japanese conditions:

a) Environmental Administrative Management and Local Government

Environmental pollution is closely related to the local environment. Therefore, the local government is responsible for the environmental administrative management and authority.

b) Ordinance of Local Government

An environmental standard is promulgated for the protection of human health from air pollution and for the preservation of the living environment, ensuring for uniformity throughout the Country. Additionally, the emission standard is stipulated to control the amount of smoke and soot dispersing from industrial activities. However, if the preservation of the living environment is inadequate, as judged from natural and social conditions, local ordinances, standards which are more stringent than national standards (override-standards) can be established.

c) Prompt Relief to Victims

The function of conciliation committee on environmental pollution at the Prime Minister's House, and the legislation for compensation for health damage caused by air pollution are effective due to the prevention of human health damage caused by air and water pollution, and provide prompt and fair relief given to the victims.

d) Polluter Pays Principle

The main problem is who should bear the environmental liability for pollution. The laws related to cost allocation law in Japan stipulate that the costs incurred in pollution control for public works are to be paid by responsible entities in an amount proportional to their contribution to the source of pollution.
- Pollution-related Health Damage Compensation Law
- Pollution Control Public Works Cost Allocation Law

e) Environment Impact Assessment (EIA)

The Environmental Impact Assessment Ordinance will come into effect from June

1999 in Japan. Even before this ordinance becomes effective, the environmental impact assessment has been actually practiced for the preservation of the environment. EIA has been practiced effectively by ordinance in local government and the Cabinet Council at the central government level, primarily in the development of large-scale industrial projects. By implementing this ordinance, it can be expected that more environmental concerns will be given towards industrial planning.

f) Laws for Optimum Location of Factories

Factory location law is established to preserve the environment and arrange proper location of factories. The industrial relocation promotion law is practiced to relocate factories from an excessively congested area to improve the environment. This law promoted facilitated the separation of industrial areas from residential areas and resulted in the improvement of environment.

- Factory Location Law
- Industrial Relocation Promotion Law

g) Effort in Greening of Industrial Production System

- Law Concerning the Improvement of Pollution Prevention System

h) Qualified Person for Heat Management

Qualified Person for Heat Management is accredited by a national examination based on the law concerning the rational use of energy. The conservation of energy is a powerful method against air pollution.

- Law Concerning the Rational Use of Energy in Specified Factories

i) Legislation of Chemical Substances

To ensure security in the use of chemical substances, there are a number of control laws related to environmental preservation.

- Drugs, Cosmetics and Medical Instruments Law
- Agricultural Chemical Control Law
- Law Concerning Control of Examination and Manufacturing of Chemical Substances
- Food Hygiene Law
- Pharmaceutical Affairs Law

The industries using large amounts of chemicals are making self-effort towards environmental preservation. The method with less emissible care is effective in order to prevent leakage and permeation of chemicals in a manufacturing process.

j) Technological Assessment

There are a number of analytical study committees in Japan, which are equivalent to the OTA (Office of Technology Assessment) in the US, for the purpose of technological analysis of environmental preservation and safety technology.

k) Legislation for Monitoring

Monitoring and analytical facility for environment and standardization of analysis law
- Industrial Standardization Law
- Measurement Law

l) Investment in Pollution Control Facility

The cumulative investment for environmental control totaled 9.8 trillion-yen during 20 years from the year of 1970 to 1990 under the various tax-exempt laws for private sectors. The R&D investment was 2.6 trillion-yen. Aggressive investment programs were instituted toward the conversion of liquefied natural gas for coal burning power plants and hydro-desulfurtization of fuel oil.
- Flue gas de-SOx: 2,173 units/209.8 million Nm^3/hr
- Flue gas de-NOx: 956 units/292.8 million Nm^3/hr and as of 1993

m) Pollution Control Agreement

Pollution Control Agreement was initially signed between local governments (prefectures and municipality) and industries (regulated entity or a group of entities). The residents joined in later in the signing of agreement. There were 37,500 agreements in 1994. The agreement was not made by compliance to law but by a mutual agreement among signing partner. The number of agreements has increased further. The agreement which covered the original seven interests (air pollution, water pollution, noise, vibration, offensive odor, soil contamination and ground subsidence) has shifted to include areas such as ecology, amenity, greening and recycling of resources.

n) Pollution Control Manager

The Pollution Control Manager System provides for the installation of pollution control systems within factories to meet the regulated levels, which was enforced by reorganization of the pollution-related law. There are 650,000 accredited pollution control managers certified by the national board today in Japan. They are involved

with environmental control (air pollution, water pollution, noise and vibration) in industries. The CEOs of the industries are responsible as supervisor of pollution control. The pollution control managers not only work as coordinators for pollution control groups but also are involved in measurements, preparation of reports, selection of raw materials, designing of control facilities, and preparation and submission of reports to the related agencies.

o) Financial Subsidiary Institution

The installation of pollution controls facilities is difficult for small and medium size industries whose financial bases are not solid enough. In such cases, provincial autonomy establishes a financial subsidiary institution and makes an effort to promote the establishment of the control facility. This institution is successful because of renting with the low interest and supplying interest by a financial subsidiary.

5.5.2 Recommendation for Pollution Control for Macedonia

(1) Revision of monitoring methods for determination of air pollution concentrations which are essential for establishment of environmental standards

The current air pollution prevention law established 13 environmental standards. However, continuous monitoring is applied to only SO_2 and TSP. After cross checking with SO_2 standard gas, the concentration of SO_2 was found lower by 20% than the previously recorded values. Based on this observation, continuous monitoring along with dynamic calibration with standard gas is desirable.
Dynamic calibration was one of the subjects offered in technology transfer during the Site Work I and II. The monitoring instruments provided by the Study were enable to satisfy the EU Directives on air pollution monitoring. Air pollution was understood easier than the previously used monitoring method. By taking advantage of the new monitoring system, the monitoring method should be modified so that prompt response to serious pollution conditions can be achieved by referring to the standards of EU Directives and WHO. It is recommended to establish environmental standards suitable for Macedonia.

(2) Operation and Management of Monitoring System

The Skopje City Assembly established an alarm announcement standard in October,

1990, based on the air pollution prevention law. The announcement of alarm is invoked in case an inversion is produced and continues more than 24 hours with an average wind velocity of less than 2 m/s or that meteorological conditions are predicted to continue for more than 24 hours. Upon collecting these data, it is necessary to establish and operate the monitoring system capable of judging the alarm criteria accurately. The details of monitoring system are summarized in Chapter 6.

(3) Operational Improvement of Environmental Impact Assessments

Because existing data of the Initial Environmental Examination (IEE) and the actual values have not been evaluated, the environmental impact assessment is not performed completely, although EIA is enacted.
It is also recommended not only to screen documents formally but also to establish EIA, including participation and agreement of residents.

- Selection of project type necessary for EIA
- Development of EIA methodology for the development activity impacting the environmental capacity

(4) Establishment of Air Pollution Control Facilities and Tax Incentives

Although a dust collector is installed at both cement and heating plants, the concentration of black soot is high. It is therefore desirable to improve the efficiency of pollution control facilities or to apply more effective new facilities. At the same time the establishment for tax-exempt incentives is also desirable for the installation of the facility. The facility countermeasures for emission sources at the small- and medium- sized industries are not satisfactorily prepared. It is desirable to support and promote these industries for the establishment of air pollution control facilities through long-term, low rate financing and a supplement of interest by a financial subsidiary.

(5) Public Relations to the Citizenry

In order to improve the environmental issues, it is greatly important to spread the importance of environmental preservation and urge the citizen to awaken to it. The public relations to the citizenry are a means for that purpose, and in many cases, the mass media such as radio, TV, and newspaper are very effective.

The MOE has already announced the conditions of air pollution to the mass media if required, and it is expected that such public relations will be more promoted. For example, opening of web-site via Internet, which has recently become popular, seems to be effective.

Positive actions for public relations are desirable so that the citizens understand the importance of environmental issues properly.